

# MACHINELEARNINGLM<sup>†</sup>: SCALING MANY-SHOT IN-CONTEXT LEARNING VIA CONTINUED PRETRAINING

Haoyu Dong<sup>\*</sup>, Pengkun Zhang, Mingzhe Lu, Yanzhen Shen, Guolin Ke

UCAS, SCUT, Stanford

donghaoyu22@mails.ucas.edu.cn

## ABSTRACT

Large language models (LLMs) possess broad world knowledge and strong general-purpose reasoning ability, yet they struggle to learn from *many* in-context examples on standard machine-learning (ML) tasks—i.e., to leverage many-shot demonstrations purely via in-context learning (ICL) without gradient descent. We introduce MACHINELEARNINGLM, a *portable continued-pretraining framework* that equips a general-purpose LLM with *robust many-shot ICL capability* while preserving its general knowledge and reasoning for broader chat workflows.

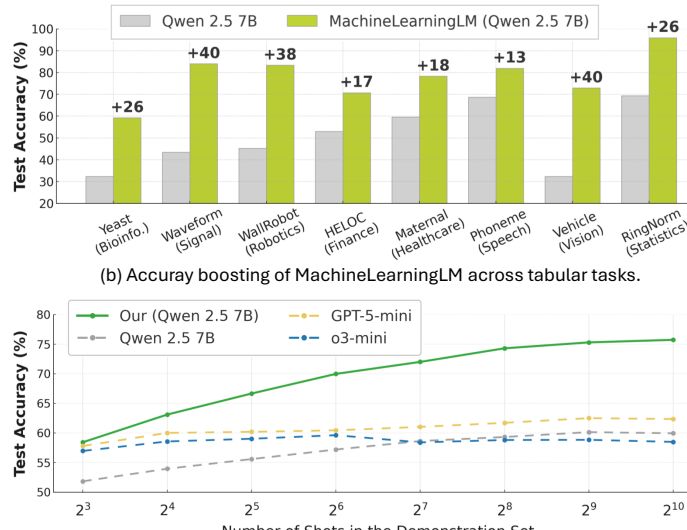
Our pretraining procedure synthesizes ML tasks from *millions of structural causal models (SCMs)*, spanning shot counts up to 1,024. We begin with a random-forest teacher, distilling tree-based decision strategies into the LLM to strengthen robustness in numerical modeling. All tasks are serialized with a *token-efficient prompt*, enabling 3–6 $\times$  more examples per context window and delivering up to 50 $\times$  amortized throughput via batch inference.

Despite a modest setup (*Qwen-2.5-7B-Instruct* with LoRA rank 8), MACHINELEARNINGLM *outperforms strong LLM baselines* (e.g., GPT-5-mini) by an average of  $\sim$ 15% on out-of-distribution tabular classification across finance, physics, biology, and healthcare domains. It exhibits a *striking many-shot scaling law*: accuracy increases monotonically as in-context demonstrations grow from 8 to 1,024. Without any task-specific training, it attains *random-forest-level* accuracy across hundreds of shots. General chat capabilities—including knowledge and reasoning—are preserved: it achieves 75.4% on MMLU.

👉 **Model & Data:** <https://huggingface.co/MachineLearningLM>  
 ↗ **Code:** <https://github.com/HaoAreYuDong/MachineLearningLM>



(a) Prompt template of MachineLearningLM.



(b) Accuracy boosting of MachineLearningLM across tabular tasks.  
 (c) Many-shot scaling of MachineLearningLM, averaged across tasks.

Figure 1: MACHINELEARNINGLM on in-context ML tasks: (a) prompt template; (b) 512-shot accuracy across domains vs. Qwen-2.5-7B-Instruct; (c) many-shot scaling ( $2^3$ – $2^{10}$  shots) vs. LLMs.

<sup>†</sup>At present, MACHINELEARNINGLM targets tabular ML; broader ML is future work.

<sup>\*</sup>Corresponding author.

## 1 INTRODUCTION

LLMs possess broad world knowledge, general perceptual as well as reasoning abilities, making them promising few-shot learners (Brown et al., 2020). However, they often fail to learn new tasks despite being given many-shot demonstrations on standard ML benchmarks (Agarwal et al., 2024; Gardner et al., 2024), or to fully exploit rich experiences stored in agent memory in interactive, open-ended workflows (Wang et al., 2023; Shinn et al., 2023; Wang et al., b). In addition, accuracy gains typically plateau—often after just a handful of demonstrations—and are sensitive to the label biases and choice/order of examples (Chen et al.; Liu et al., 2024a; Zhao et al., 2021; Fei et al., 2023; Liu et al., 2022). In practice, LLMs are largely guided by surface-level signals, such as distributional, formatting cues (Min et al., 2022) and nearest-neighbor imitation (Agarwal et al., 2024), and rarely uncover new causal mechanisms or statistical dependencies that are required to yield accurate predictions.

Orthogonally, pioneering tabular models (Hollmann et al., 2025; Qu et al., 2025) have demonstrated ML tasks can be solved purely by ICL—*without gradient descent*. However, these tabular-specific model architectures cannot leverage the broad prior world knowledge and general-purpose multimodal perception that LLMs acquire during pretraining; consequently, they depend heavily on well-designed featurization (Shi et al., 2021; Mráz et al., 2025) and abundant labeled data for training. At this intersection, we ask:

***Can we teach an LLM to “do ML in context” while preserving general abilities?***

To this end, we propose a *pretraining-plus-prompting* framework, MACHINELEARNINGLM, that equips LLMs with in-context ML capabilities to fully exploit many-shot in-context examples. MACHINELEARNINGLM performs LoRA-based (Hu et al., 2022) continued pretraining with a standard next-token objective on millions of *synthetic* tabular prediction tasks drawn from SCM-based priors (Peters et al., 2017; Pearl, 2009): a task generator samples arbitrarily large numbers of binary/multiclass tasks under SCM-based priors spanning diverse feature types, marginal distributions, and label mechanisms following (Qu et al., 2025). This approach ensures strict non-overlap between our pretraining data and evaluation datasets. After pretraining, the model can directly leverage in-context examples of a new task to generate predictions for unseen instances—*without* parameter update.

As summarized in Table 1, unlike previous instruction-tuning methods (Wang et al., 2022b; Chung et al., 2024) that rely on a limited set of real tasks (typically  $\sim 10^3$ ), we train on  $\mathcal{O}(10^6)$  synthetic tasks with *diverse causal mechanisms and varied shot counts*. Our approach also differs from specialized tabular learners as we preserve the versatility of LLMs, which enables them to continue to leverage contextual task descriptions, draw on external knowledge, and interact directly with multimodal, heterogeneous inputs. Through large-scale pretraining, our method is able to equip LLMs with striking many-shot scaling and robust numerical modeling. We hope MACHINELEARNINGLM is a promising paradigm to inspire new research that leverages LLMs’ general perception and reasoning capabilities, and also possibly extending to more modalities beyond text, as detailed in Section 6.

Table 1: Comparison across ML paradigms.

Method	In-context learning	Robust numerical modeling	General knowledge priors	Native multimodal input
RF, Boosted trees	✗	✓	✗	✗
TabPFN, TabICL	✓	✓	✗	✗
TabLLM	✗	✗	✓	✓
GPT-5, Qwen	✓	✗	✓	✓
MACHINELEARNINGLM	✓	✓	✓	✓

**Key:** ✓ Yes, ✗ No. **Note:** “Native multimodal” primarily means *textual + numerical + tabular* and can be naturally extended to modalities like images by building on multimodal LLM backbones.

**Warm-up training with a Random Forest teacher.** Directly training on synthetic tasks can lead to model collapse or underperformance, particularly when tasks are too complex to be learned from only a few (e.g., 64) examples. This makes strong ML methods no better than random guessing or always predicting the majority class. We stabilize the onset by *mimicking a random-forest (RF) teacher* on each task—first matching example predictions—before transitioning to self-reliant in-context prediction. This leverages knowledge distillation for improved optimization (Hinton et al., 2015). We choose a random forest teacher for its balance of robustness and interpretability. Its decision process can be transparently decomposed into rule paths and feature attributions and directly serialized into interpretable “reasoning steps”—then rule chains and faithful local explanations (Deng, 2014; Friedman & Popescu, 2008; Lundberg & Lee, 2017), which naturally align with the chain-of-thought (CoT) reasoning. In this work, we distill the predicted labels only, but future directions could leverage its “reasoning steps” as rationales for reasoning-augmented training (Guo et al., 2025) and enhancing the interpretability of model predictions.

**Token-efficient prompting for in-context ML.** LLMs are fundamentally bottlenecked by their context length. Our design *enables 3-6 $\times$*  more examples within a context window and yields 50 $\times$  amortization via batch inference. We achieve this with three composable design choices.

- (i) A *tabular encoding* to organize many-shot examples rather than as *scattered and lengthy* NL descriptions (Hegselmann et al., 2023; Gardner et al., 2024). Recent works (Dong et al., 2024; Sui et al., 2024) have shown that regular tabular structures can be seamlessly understood by LLMs without requiring special row/column attention (Hollmann et al.). In addition, tabular encoding<sup>1</sup> naturally combines *heterogeneous* with no mandatory categorization for text.
- (ii) A *compact integer-based encoding* in which we normalize all numbers for each numerical feature to integers in [0, 999], eliminating the tokenization fragmentation caused by decimal points (“.”) and leading signs (“+”/“-”). This not only reduces the token count—e.g., `c1100k_base` treats any integer in [0, 999] as a single token, but also avoids a common pitfall where LLMs compare decimals as strings (e.g., “1.11” (1 | . | 11) vs. “1.9” (1 | . | 9)) (Hugging Face, 2024).
- (iii) A *sequence-level batch-prediction* mechanism that packs dozens of test examples into each sequence and predicts all of them in a single forward pass, stabilizing gradients for continued pre-training and amortizing instruction/context overhead (Lin et al.; Cheng et al., 2023).

**Order-robust, confidence-aware self-consistency.** LLM predictions can be sensitive to long-context position effects (Liu et al., 2024a). At inference, we marginalize over permutations of demonstration and feature order, combining outputs via *confidence-weighted self-consistency*—i.e., a calibrated, probability-weighted vote over samples (Zhao et al., 2021; Wang et al., a).

MACHINELEARNINGLM continues pretraining on millions of synthetic tasks with diverse causal mechanisms and varied shot counts; our **key experimental highlights** are:

- **Many-shot scaling.** MACHINELEARNINGLM exhibits striking many-shot scaling across diverse tasks from the TALENT benchmark (Liu et al., 2024b), surpassing both leading open-source (e.g. Qwen-2.5-7B) and closed-source (e.g. GPT-5-mini) LLMs by an average of  $\sim 15\%$  under high-shot settings. Moreover, it exhibits clear out-of-distribution generalization in context length, from a 32k-token pretraining budget to a 131k-token inference budget.
- **Competitive many-shot performance vs. state-of-the-art tabular methods.** Without any task-specific training, MACHINELEARNINGLM reaches *random-forest-level* accuracy across shot counts from 8 to 512 (within 2% *relative* on average) and clearly surpasses instance-based kNN, demonstrating robust numerical modeling.
- **Heterogeneous (multimodal)-input generalization.** By combining LLM versatility with classical ML’s robust numerical fitting, MACHINELEARNINGLM natively consumes natural-language (NL) features alongside numerical values—*without relying on text bucketing or embeddings*—and achieves competitive results on the Talent benchmarks.

<sup>1</sup>It is extensible and can support images, hyperlinks, and embedded objects, as in HTML tables.

- **General abilities preserved (chat workflows).** MACHINELEARNINGLM retains general capabilities in chat-style workflows; for example, on MMLU it attains 73.2% micro accuracy in 0-shot and 75.4% in 50-shot, comparable to strong general-purpose LLMs.

## 2 METHOD

### 2.1 PRETRAINING CORPUS SYNTHESIS

To generate pretraining data, we build a task generator following TabICL<sup>2</sup> (Qu et al., 2025) that samples diverse binary/multiclass problems under SCM-based priors determined by choices of graph structure, mechanisms, feature types, and class formation.

**SCM graph and mechanisms.** We first sample a DAG  $\mathcal{G}$  following the structure of a fully connected MLP, where each neuron corresponds to a variable, then assign structural equations to each node  $v$  in  $\mathcal{G}$ :

$$x_v \leftarrow f_v(x_{\text{parents}(v)}) + \varepsilon_v, \quad \varepsilon_v \text{ i.i.d. noise.}$$

where  $f_v$  is drawn from a rich pool of functions, following (Qu et al., 2025), including *tanh*, *leaky-ReLU*, *ReLU*, *ReLU6*, *SELU*, *SiLU*, *Softplus*, *Hardtanh*, *sign*, *sine*, *RBF*, *exp*, *gaussian-process-sampled random activations*,

**Tree-based SCMs.** To inject tree inductive biases beyond neural layers, 30%  $f_v$ s are replaced by multi-output gradient-boosted regressors ( $f_\ell$ ) fitted on fake targets drawn from Gaussian noise and parent inputs. For each layer:

$$n_{\text{estimators}} \sim \min\{4, 1 + \text{Exponential}(\lambda = 0.5)\},$$

$$\text{max\_depth} \sim \min\{4, 2 + \text{Exponential}(\lambda = 0.5)\},$$

We also fit  $f_\ell : x_{\text{parents}(\ell)} \mapsto y$  with  $y \sim \mathcal{N}(0, I)$ ,

and set  $x_\ell \leftarrow f_\ell(x_{\text{parents}(\ell)})$ .

**Feature and label typing.** We sample a fraction of categorical features, discretize dense columns into bins, and (with some probability) shuffle category IDs to avoid spurious order. Continuous features remain numeric. As for a scalar  $y^*$ . We create  $K$ -way labels by sampling  $K \in \{2, \dots, 10\}$ , drawing ordered bounds  $\tau_1 < \dots < \tau_{K-1}$  from the empirical distribution of  $y^*$ , and mapping

$$y = \arg \max_{k \in \{1, \dots, K\}} \mathbb{1}[\tau_{k-1} \leq y^* < \tau_k],$$

Followed by a random permutation of class IDs to destroy ordinal hints. Class imbalance arises naturally from the sampled bounds.

**Task sampling policy and corpus scale.** We repeatedly instantiate fresh SCMs, yielding a corpus of  $\sim 3 \times 10^6$  distinct SCMs. For each SCM, we propagate noise through the structural equations to generate i.i.d. samples  $(X, y)$ . For each task, we sample the number of demonstrations  $M$  (capped at 1,024), fix the number of queries at  $N = 50$ , and draw the number of features  $d \in \{5, \dots, 50\}$  and classes  $K \in \{2, \dots, 10\}$ . Each task is serialized into a prompt following Section 2.4 and comprises the following components: a compact tabular many-shot block (features with labels), a tabular test block (IDs with features), and an instruction specifying a JSON array output  $[{"id": \cdot, "label": \cdot}, \dots]$ , as illustrated in Figure 1a. Given a token budget of 32k Qwen 2.5-Instruct in our framework, we truncate the number of many-shot samples per task to fit the length limitation for continued pre-training.

<sup>2</sup>We directly use the source code of TabICL in <https://github.com/soda-inria/tobicl>.

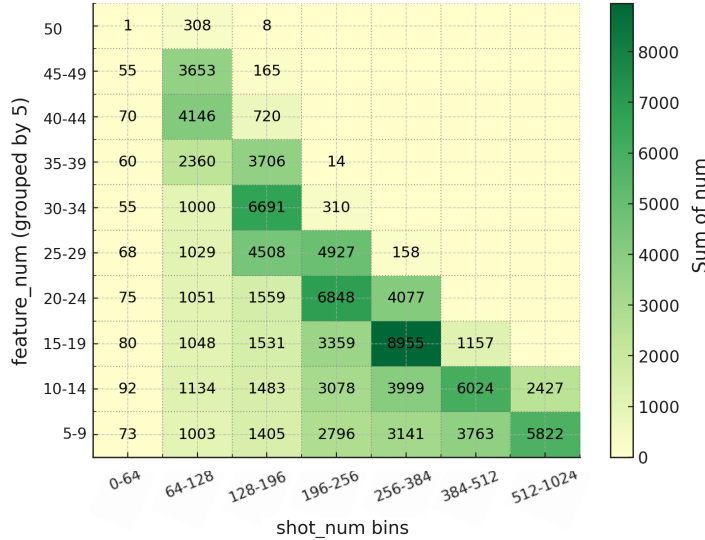


Figure 2: Heatmap of task density across feature and shot counts. We sample 100k tasks from the synthetic generator and aggregate by `feature_num` and `shot_num` bins. Color encodes the sum of `num` per bin. Training token budget capped at 32k tokens.

## 2.2 OBJECTIVE OF CONTINUED PRE-TRAINING

As illustrated in Figure 1a, we cast each in-context tabular prediction task as a *conditional sequence modeling* problem. For a given task, the prompt  $x$  concatenates: (i) an instruction *header*  $H$  describing the task and specifying a JSON output format, (ii) a many-shot training block with a *demonstration block*  $S = \{s_i\}_{i=1}^M$  of  $M$ -shot labeled demonstrations (demonstration order immaterial), and (iii) a *query block*  $Q = \{x^{(i)}\}_{i=1}^N$  of  $N$  unlabeled queries (each with an `id`). (ii) and (iii) follow the token-efficient prompting in Sec. 2.4.

$$\underbrace{H}_{\text{instruction + schema}} \parallel \underbrace{s_1 \parallel \cdots \parallel s_i \parallel \cdots \parallel s_{M-1}}_{\text{in-context demonstrations}} \parallel \underbrace{x_1 \parallel \cdots \parallel x_{N-1}}_{\text{batched queries}}$$

The model is required to generate a single JSON array.

$$y = [\{"id": 0, "label": \hat{l}_1\}, \dots, \{"id": N-1, "label": \hat{l}_{N-1}\}].$$

**Loss.** We introduce no auxiliary heads or bespoke objectives, and use the standard left-to-right log-likelihood language modeling objective *over the JSON target* for continued pre-training. Formally, let  $\text{tok}(\cdot)$  denote the tokenizer and

$$\mathbf{x} = \text{tok}(x), \quad \mathbf{y} = \text{tok}(y) = (y_1, \dots, y_T).$$

The training loss for parameters  $\theta$  is the negative log-likelihood

$$\mathcal{L}(\theta) = - \sum_{t=1}^T \log p_\theta(y_t \mid \mathbf{x}, y_{<t}), \quad (1)$$

applied to the *entire* JSON string (brackets, keys, colons, commas, IDs, and label tokens). This encourages (i) learning the mapping from features to labels, (ii) preserving test-row order via aligned `"id"` fields, and (iii) strict adherence to the required JSON format.

## 2.3 RANDOM-FOREST MIMIC WARM START

Directly training on synthetic tasks can cause training collapse as low-signal tasks, limited few-shot examples, severe class imbalance, and randomly sampled label regimes may yield poor local optima,

bend the loss curve, and occasionally destabilize training (Ochal et al., 2023). We mitigate this risk by first *mimicking a Random Forest (RF) teacher* on each task, where we match per-example predictions in a short warm-up—before transitioning to standalone in-context prediction. This provides more informative targets and smoother gradients in the early phase, similar to knowledge distillation (Hinton et al., 2015). We choose RF as the teacher because its decision process decomposes transparently into rule paths and feature attributions. These can be serialized as explicit “reasoning steps” (Deng, 2014; Friedman & Popescu, 2008; Lundberg & Lee, 2017), which aligns naturally with the stepwise reasoning patterns large language models can emulate.

For each pretraining task, we (i) utilize a *better-than-random guard* at the task level to skip low-signal or degenerate tasks, and (ii) apply an *example-level consensus filter* that retains only test examples where the RF prediction matches the ground truth; we filter examples at this stage but *do not* alter the original train/test labels. After the warm-up ends, we continue to apply (i) but *disable* (ii), enabling the model to transition from relying on random-forest-induced priors to developing its own in-context ML behavior. This design prunes low-signal tasks before they corrupt optimization and, by supplying high-precision targets, reduces gradient noise, prevents collapse-to-majority under imbalance, and yields a smoother warm-up that mimics robust numerical modeling—ultimately easing the shift from teacher imitation to independent in-context ML.

**(i) Task-level guard against chance and collapse.** To rule out degenerate tasks where the RF performs no better than chance, we compare its accuracy to a conservative random baseline

$$p_0 = \max\left(\sum_{k=1}^K p_k^2, \max_k p_k\right),$$

where  $K$  is the number of classes, and  $p_k$  denotes the class prior from  $y_{\text{true}}$ . This baseline corresponds to the larger of “sampling by prior” or “always predicting the majority class.” Let  $N_{\text{correct}} = \#\{i : y_i = \hat{y}_i\}$  be the number of correct predictions, we then perform a one-sided binomial tail test  $p\text{-value} = \Pr[X \geq N_{\text{correct}}]$ ,  $X \sim \text{Bin}(N, p_0)$  and require  $p\text{-value} < \alpha$ .<sup>3</sup>

To avoid trivial solutions and collapsed behavior under class imbalance, we enforce the following criteria<sup>4</sup>—each targets a distinct failure mode:

- **Chance-corrected agreement:** Cohen’s  $\kappa > 0$ .
- **Imbalance-robust accuracy:** Balanced accuracy  $> 1/K + \delta_{\text{bacc}}$ .
- **Macro-F1 dominance:**  $F1_{\text{macro}} \geq F1_{\text{macro}}^{(\text{maj})} + \delta_{\text{F1}}$ .
- **Non-collapse checks:** At least two predicted classes; dominant predicted class fraction  $\leq \tau_{\text{dom}}$ .
- **Evaluation setup:**  $N = 50$  and  $K \geq 2$ .

Tasks failing to meet all criteria are *skipped*, and only tasks passing all criteria are used in pretraining.

**(ii) Example-level label-prediction consensus filter (warm-up only).** For admitted tasks, we retain in the prompt only those evaluation examples where the RF prediction matches the ground truth (RF = GT), discarding mismatched cases while keeping original labels and splits unchanged. This enforces teacher–student alignment without relabeling, yielding cleaner supervision in the earliest updates. After the warm-up stage, consensus filtering is discontinued, allowing the model to move beyond imitation and develop standalone in-context policies.

After filtering, we reduce the evaluation set size from  $N = 50$  to  $N_{\text{conse}} = 20$ . For the remaining usable examples, we resample within each label class to restore  $N_{\text{conse}} = 20$ , aiming to match the proportions of many-shot demonstrations. This prevents collapse-to-majority under imbalance and avoids sub-optimal supervision.

<sup>3</sup>For  $N = 50$  the test has relatively low power; we use a slightly relaxed  $\alpha$  (default 0.2) to avoid discarding borderline-but-promising tasks.

<sup>4</sup>We use  $\kappa > 0.01$ ,  $\delta_{\text{bacc}} = 0.03$ ,  $\delta_{\text{F1}} = 0.00$ , and  $\tau_{\text{dom}} = 0.95$ , where *maj* denotes the always-majority classifier.

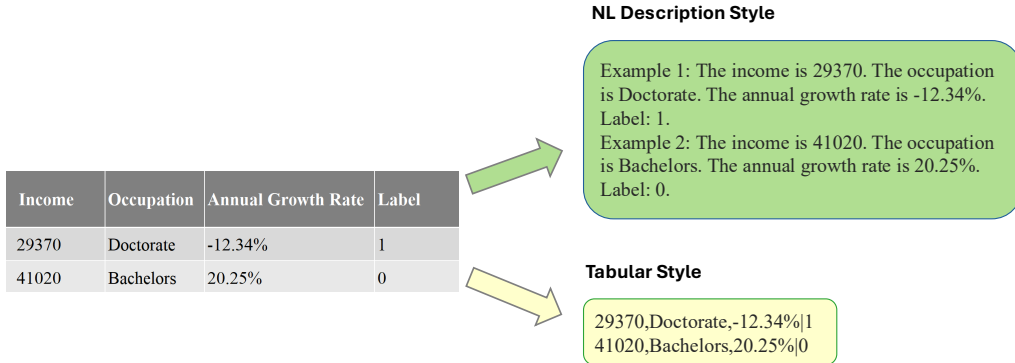


Figure 3: A comparison between the NL description style and tabular style of many-shot examples.

## 2.4 TOKEN-EFFICIENT PROMPTING FOR IN-CONTEXT ML

The application of many-shot in-context ML is often constrained by the fixed context length and high computational cost of long contexts (Gardner et al., 2024). We alleviate these limitations through three design choices: **(i)** compact structuring of in-context examples, **(ii)** compression of numeric tokens, and **(iii)** sequence-level batching.

### 2.4.1 TABULAR ENCODING

Instead of presenting demonstrations  $S$  as scattered NL descriptions (Hegselmann et al., 2023; Gardner et al., 2024), we place many-shot examples in a concise table-style format. Building on recent findings that normal tabular structures can be seamlessly understood by popular LLMs (Dong et al., 2024; Sui et al., 2024), our approach preserves column/field meaning while dramatically reducing tokens relative to full-sentence templates.

The example in 3 contrasts an encoding table expressed as scattered NL descriptions, as in TabLLM (Hegselmann et al., 2023) and TabuLa (Gardner et al., 2024). with our compact tabular encoding, where commas separate features and “|” separates the label (the header is optional).

Notably, while feature names and task descriptions may contain contextual semantics that could be readily exploited by LLMs, our approach *avoids* using such information. This ensures a fair comparison with traditional ML methods and avoids data contamination and memorization (Bordt et al.). Moreover, the current tabular encoding jointly represents heterogeneous textual and numeric features, *without requiring mandatory categorical bucketing or embedding extraction* for text. Toward future extensions of current tabular encoding to *multimodal* features, HTML tables can be leveraged to support images, hyperlinks, and embedded objects.

### 2.4.2 COMPACT INTEGRAL-BASED NUMBER ENCODING

We normalize all numbers of each numerical feature to non-negative integers in  $[0, 999]$  to eliminate the tokenization fragmentation caused by decimal points (“.”) and leading signs (“+”/“-”). The resulting values are then represented as plain text. This preserves ordinal structure yet maps each number from a sequence of scattered tokens to an integral single token under GPT’s `c1100k_base`. Beyond token savings, integer rendering avoids a frequent pitfall where decimals are compared text-wise (e.g., “1.11” (1 | . | 11) vs. “1.9” (1 | . | 9 where 11 is bigger than 9 while 1.11 is smaller than 1.9)) rather than numerically (Spithourakis & Riedel, 2018; Wallace et al., 2019; Singh & Strouse, 2024; Hugging Face, 2024).

**Connection to  $z$ -norm.** Recent work in tabular modeling, including TabICL (Qu et al., 2025), has adopted  $z$ -score normalization (mean–variance standardization) for each feature, which yields real-valued decimals. We also adopt this approach as the initial step before discretizing the normalized values into bounded integers in  $[0, 999]$ .

**Integer mapping.** We map each normalized value  $z$  to an integer  $i \in [0, 999]$  via  $i = \text{clip}(\text{round}(120z + 500), 0, 999)$ , where  $\text{round}(x) = \lfloor x + 0.5 \rfloor$  and  $\text{clip}(x, a, b) = \min\{\max(x, a), b\}$ .

Under this mapping,  $z = 0$  is mapped to  $i = 500$ , and  $z = \pm 4.166$ —which covers 99.997% of values under the standard normal distribution—maps approximately to  $i = 0 - 999$ , with out-of-band values clipped. This transformation yields  $[0, 999]$ -norm, which preserves numeric order while ensuring that most values are tokenized as a single token under `cl100k_base`. Specifically, GPT (`cl100k_base`) and LLaMA-3 vocabularies merge consecutive digits, commonly treating a sequence of three digits as a single token. In contrast, Qwen and LLaMA-2 vocabularies tokenize numbers at the level of individual digits, leading to much more fragmented representations. Below illustrates typical fragmentations of popular tokenizers for z-norm decimals and [0-999] non-negative integers.

#### Z-norm (decimal form)

<i>GPT (cl100k_base), LLaMA-3:</i>	$-0.1234 \rightarrow$	
<i>Qwen, LLaMA-2:</i>	$-0.1234 \rightarrow$	

#### [0,999]-norm (integer form)

<i>GPT (cl100k_base), LLaMA-3:</i>	486	
<i>Qwen, LLaMA-2:</i>	486	

#### 2.4.3 SEQUENCE-LEVEL BATCH-PREDICTION

As shown in Figure 1, we *pack*  $N$  query rows into a single sequence and decode all predictions in one forward pass, increasing the *effective* batch size at the sequence level (Lin et al.; Cheng et al., 2023). Let the sequence consist of a shared header  $H$  (task instruction, schema) and in-context demonstrations  $S$ , followed by  $N$  test queries  $\{x^{(i)}\}_{i=1}^N$  and an output section for predictions  $\{y^{(i)}\}_{i=1}^N$ :

$$\underbrace{H \parallel S}_{\text{instruction + schema + } M \text{ shots}} \parallel \underbrace{x^{(1)} \parallel \cdots \parallel x^{(N)}}_{\text{batched queries}} \implies \underbrace{y^{(1)} \parallel \cdots \parallel y^{(N)}}_{\text{batched predictions}}.$$

During training, **MACHINELEARNINGLM** remains purely autoregressive and is optimized with the standard next-token objective (Section 2.2). Increasing  $N$  accelerates and stabilizes continued pre-training. At inference, the model predicts  $N$  samples in a single pass, amortizing instruction and context overhead (Section 2.4.4).

**Stability and reliability.** A big  $N$  not only consumes the token budget that would otherwise be allocated to demonstrations, but also increases instruction-following errors (e.g., cross-item interference and run-on/non-terminated generations), particularly for smaller open-source models. We therefore set  $N = 50$  by default. In addition, we randomize the within-sequence order of  $\{x^{(i)}\}$  to reduce position bias and improve exchangeability of the batched items.<sup>5</sup> Importantly, `id` should be 0-indexed; 1-based indexing often destabilizes instruction following and leads to incorrect IDs.

#### 2.4.4 COMPRESSION AND AMORTIZATION RATIO

**Token-cost model.** We model the amortized token cost per predicted label as follows.

Let  $M$  denote the number of many-shot demonstrations (with labels) and  $N$  be the number of query examples to be inferred (with IDs). Each row is dominated by its  $d$  features, so we represent the per-row token cost by  $R$ , without distinguishing labels and IDs. The instruction/schema header incurs a token cost of  $H$ , which is negligible compared to  $R(M + N)$  and can be omitted. The resulting amortized token cost per predicted label is therefore

$$C = \frac{H + R(M + N)}{N} \approx \frac{R(M + N)}{N}.$$

<sup>5</sup>This simple permutation also helps mitigate long-context position effects observed in batch-prediction.

**Compression and amortization ratio.** The overall compression ratio is defined as the product of three saving factors: (A) *tabular structure*, (B) *number normalization*, and (C) *batch inference*

(A) TABULAR STRUCTURE (NL-DECIMAL  $\rightarrow$  TABULAR-DECIMAL). We replace scattered NL sentences (e.g., “the first feature is 0.1234”) with compact, comma-delimited rows, and we apply this format throughout Section 2.4.4. This will substantially reduce the per-row cost  $R$ . Counting words, spaces (absorbed into word tokens), numbers, and delimiters, we obtain:

Model / Tokenizer	$R_{\text{NL,dec}}$	$R_{\text{Tab,dec}}$	Ratio
GPT(c1100k_base), LLaMA-3	10	5	<b>2.0<math>\times</math></b>
Qwen, LLaMA-2	12	7	<b>1.71<math>\times</math></b>

(B) NUMBER NORMALIZATION. Mapping normalized decimals to the integer range  $[0, 999]$  preserves the relative rank of decimals while collapsing numbers to a single token under `c1100k_base` (and 2–3 tokens under Qwen’s tokenizer).

*Without delimiters.* For example, “0.1234” requires 4 tokens, whereas “234” requires only 1; similarly, “−0.1234” requires 5 tokens, compared to 1 for “234”. Assuming a balanced distribution of positive/negative numbers, the expected token length is  $(0.5 \times 4 + 0.5 \times 5) = 4.5$  before normalization and 1 after. Thus, the expected per-number reduction under `c1100k_base` is **4.5 $\times$** . In Qwen’s tokenizer, positives use 6 tokens vs. 3 after, negatives 7 vs. 3 after; the expected length is  $(0.5 \times 6 + 0.5 \times 7) = 6.5$  before and 3 after, giving  $6.5/3 \approx \mathbf{2.17}\times$ .

*With delimiters.* In practice, each number will be followed by a delimiter (a single-token comma), which increases numerator and denominator lengths by +1. Hence for `c1100k_base`, this yields an expected length of 5.5 before normalization versus 2 after, giving  $5.5/2 = \mathbf{2.75}\times$ . For Qwen’s tokenizer, the corresponding expectation is 7.5 before versus 4 after, resulting in  $7.5/4 \approx \mathbf{1.88}\times$ .

These expected compression ratios propagate to corpus-level savings:

Model / Tokenizer	w/o delimiters	w/ delimiters
GPT(c1100k_base), LLaMA-3	<b>4.5<math>\times</math></b>	<b>2.75<math>\times</math></b>
Qwen, LLaMA-2	<b>2.17<math>\times</math></b>	<b>1.88<math>\times</math></b>

(C) BATCH INFERENCE. Given  $C(N) = \frac{R(M+N)}{N}$ , increasing  $N$  amortizes the many-shot block.

General form:

$$\frac{C(1)}{C(N)} = \frac{N(M+1)}{M+N} \quad (\text{independent of tokenizer since } R \text{ cancels}).$$

Derivation for  $M=1024$ , from  $N=1$  to  $N=50$ :

$$\frac{C(N=1)}{C(N=50)} = \frac{50 \times (1024+1)}{(1024+50)} = 47.7 \times .$$

**Overall compression and amortization.** Since Stages (A), (B), and (C) are independent, their effects compound multiplicatively. From a compression perspective, (A) structural formatting and (B) number normalization compound multiplicatively to shrink the per-row token cost  $R$ , which then will allow the LLM context to accommodate more many-shot demonstrations.

Hence *Compression* ( $a \times b$ ):

$$\text{GPT(c1100k_base), LLaMA 3: } 2.0 \times 2.75 \approx \boxed{5.5 \times}, \quad \text{Qwen, LLaMA 2: } 1.71 \times 1.88 \approx \boxed{3.2 \times}.$$

*Amortization* ( $c, n=50$ ):

$$\boxed{47.7 \times}$$

Notably, the above estimate assumes that the prompt header  $H$  contributes negligibly to the overall computation. Beyond this estimation, we leverage our SCM-based synthetic pretraining corpus to

evaluate the amortized token cost per inference sample using both our encoding and TabuLa (Gardner et al., 2024)’s. Under this setup, we observe a 136 $\times$  improvement using Qwen’s tokenizer.

## 2.5 ORDER-ROBUST, CONFIDENCE-AWARE SELF-CONSISTENCY AT INFERENCE TIME

Our approach is similar to self-consistency proposed by (Wang et al., 2022a), but modifies both the source of diversity and the aggregation method. Instead of generating diverse reasoning paths from identical prompts via stochastic sampling, we create diversity by shuffling in-context demonstrations or features across prompt variants. We then aggregate the model’s responses using weighted majority voting (Littlestone & Warmuth, 1994) to select the most consistent prediction.

More specifically, given a prompt with  $M$  in-context demonstrations, we generate  $V$  shuffled variants  $\{P_0, P_1, \dots, P_{V-1}\}$  and obtain the model’s next-token probabilities for each variant via parsing responses of LLMs. For each query, we extract the corresponding probability of the next token for each possible label  $y_j \in \{y_1, y_2, \dots, y_k\}$  from the model’s vocabulary distribution. For prompt variant  $P_i$ , let  $p_i(y_j)$  denote the probability assigned by the LLM to the token representing label  $y_j$  as the next token in the sequence. We compute the aggregate probability for each label by summing across all prompt variants:

$$\tilde{p}(y_j) = \sum_{i=0}^{V-1} p_i(y_j) \quad (2)$$

The final prediction is then determined by selecting the label with the highest aggregate probability:  $\hat{y} = \arg \max_{y_j} \tilde{p}(y_j)$ . We set  $V = 5$  in the following experiments—far fewer than the 32 used by TabICL and TabPFN.

## 3 EXPERIMENTS

### 3.1 PRELIMINARY

#### 3.1.1 EVALUATION DATASETS

We evaluate on the TALENT benchmark (Ye et al., 2024), which comprises 200 classification tasks, several of which include both tabular and textual features. For the main study, we select 32 datasets via domain clustering and sampling, and add 86 more as an extended set. We exclude one dataset whose combined numerical and textual fields exceeded our context-length budget. All tasks are listed in the Appendix. Each dataset is split 80/20 into train/test, and we report accuracy (ACC).

#### 3.1.2 BASELINES

**Tree-based learners.** We include classical tree ensembles as strong tabular baselines: Random Forest (RF) (Breiman, 2001), LightGBM (Ke et al., 2017), XGBoost (Chen & Guestrin, 2016), and CatBoost (Prokhorenkova et al., 2018). In our main comparisons, we report *Random Forest* because it is stable and robust from few-shot to many-shot regimes and easy to reproduce at scale. We use the same hyperparameters as the RF teacher in the LLM experiments. For Random Forest, we set `n_estimators=30`, `fix_random_state` for determinism, and use `n_jobs=8` (we already parallelize across processes).

**Instance-based learner.** Recent work by Agarwal et al. (2024) suggests that LLMs can behave similarly to local neural networks when learning linear high-dimensional functions with numerical inputs. Motivated by this observation, we include  $k$ -nearest neighbors ( $k$ NN) (Cover & Hart, 1967) as a simple instance-based baseline. Specifically, we use `n_neighbors=8`, `weights="distance"`, and the Minkowski distance with  $p=2$ .

**Tabular ICL models.** We compare to **TabICL** (Qu et al., 2025), a recent in-context learners for tabular data. We run their public ICL-style inference (no gradient updates), which is faster to evaluate and aligns with our in-context setup. We also compare against **TabuLa-8B** (Gardner et al., 2024), an 8B LLM fine-tuned specifically for tabular prediction.

**General-purpose LLMs.** For closed-source LLMs, we evaluate **GPT-5-mini** (latest public snapshot) and the reasoning-oriented **o3-mini** (OpenAI, 2024; 2025). For open-source LLMs, we use **Qwen-2.5-7B-Instruct** (Bai et al., 2023) as a strong lightweight baseline. MACHINELEARNINGLM is also built on Qwen-2.5-7B-Instruct via continued pretraining, enabling a direct apples-to-apples comparison under identical prompting.

### 3.1.3 CONTINUED PRETRAINING SETTING INTRODUCTION

We employ the task generator described in Section 2.1 to construct our synthetic pretraining corpus. Our dataset comprises 3 million synthetic tasks, each containing no more than 1,024 samples with feature dimensions ranging from 5 to 50 and up to 10 class labels. Owing to the 32k-token context limit during training, we truncate the number of in-context examples per task during continued pretraining.

We build upon Qwen-7B-Instruct (Bai et al., 2023) as our backbone model, which utilizes rotary positional embeddings. We adopt a two-stage continual pretraining approach, implemented using LoRA (Hu et al., 2022) with rank 8 over attn+MLP and the Adam optimizer (Kingma & Ba, 2014), within the LLaMAFactory framework (Zheng et al., 2024). Training was distributed across 5 nodes with 40 A100 GPUs, achieving a throughput of 300 tokens per second (100s per iteration, with each iteration processing  $\sim$ 30k tokens). We set lr\_scheduler\_type as cosine to use the cosine learning rate scheduler throughout training. In the first (warm-up) stage, we set the learning rate to  $1 \times 10^{-5}$  and trained on approximately 1 million tasks over 100 hours. The second stage resumed from the Stage 1 checkpoint with a reduced learning rate of  $1 \times 10^{-6}$ , continuing on about 2 million tasks for 200 hours. We set the batch size per GPU to 1, and updated model parameters every 8 steps. With 40 GPUs, this corresponds to one parameter update per 320 samples.

### 3.1.4 TEST TIME SETTING

For ICL evaluation, we partition test data into chunks of size  $N$ , with each chunk serving as a test batch. For each test chunk, we randomly sample  $M$  training examples as in-context demonstrations, and we use different sets of  $M$  examples for each batch to ensure the results are not biased by a particular fixed set. When generating prompt variants as described in Section 2.5, we shuffle only the order of the  $M$  in-context examples while keeping the test examples and their order fixed. For fair comparison with traditional ML models, we randomly sample  $M$  training examples for model training and evaluate on the complete test set, as detailed in our public code.

Importantly, although the header row in tabular data could be used to incorporate feature names/descriptions that LLMs could easily leverage (Bordt et al.), our method *intentionally excludes such information* during training and inference. This design choice promotes a fair comparison with conventional machine learning approaches and mitigates risks of data leakage and memorization (Bordt et al.), while still delivering competitive performance. Additionally, our current tabular encoding strategy jointly models both textual and numerical features, without relying on categorical bucketing or explicit text embedding extraction. The number of  $S$  samples for voting is 5 due to computational constraints, while TabICL and TabPFN use 32.

## 3.2 EXPERIMENT RESULTS

### 3.2.1 MACHINELEARNINGLM VS. VANILLA LLMs

As Table 2 and Table 3 show, pretraining solely on synthetic tabular tasks yields *large, consistent* gains over vanilla LLMs. Averaged across tasks, MACHINELEARNINGLM improves absolute accuracy of the backbone Qwen-2.5-7B-Instruct model by  $\sim$ **15%** (Table 2), with about  $\sim$ 50% of tasks seeing 15% improvements across finance, biology, vision, speech, robotics, statistics, and healthcare domains (Table 3); virtually no task exhibits a marked degradation (Table 3). At high shot counts (128–1,024), MACHINELEARNINGLM *surpasses GPT-5-mini* by  $\sim$ **12%** and o3-mini by  $\sim$ **16%** on average (cf. Figure 1c and Table 2). More results on extended tasks are presented in Appendix C.

Table 2: Test accuracy (%) across number of shots  $M=8\text{--}512$ . Notably, as shown in Figure 2, a large fraction of training tasks exceed the 32k-token limit when both the number of shots  $M$  and number of features  $K$  are big; nevertheless, the model exhibits out-of-distribution generalization to 131k-token contexts. Abbreviations: Qwen-7B=Qwen-2.5-7B-Instruct; Ours=MArCHINELEARNINGLM (base: Qwen-2.5-7B-Instruct).

Number of shots	Not in-context learning		In-context learning				
	KNN	Random Forest	TabICL	GPT-5 mini	o3-mini	Qwen-7B	Ours
8	55.3	59.1	57.4	57.8	57.0	51.8	58.4
16	60.1	63.5	64.0	60.0	58.6	53.9	63.1
32	63.4	68.0	68.6	60.2	59.0	55.6	66.7
64	65.9	71.4	72.6	60.4	59.6	57.2	70.0
128	68.1	74.3	76.0	61.0	58.4	58.6	72.0
256	69.5	76.1	79.1	61.7	58.8	59.3	74.3
512	71.1	77.7	80.9	62.5	58.8	60.1	75.3

### 3.2.2 MANY-SHOT SCALING

MArCHINELEARNINGLM displays a *striking many-shot scaling law*: accuracy increases monotonically as we raise the in-prompt demonstrations from  $2^3$  to  $2^{10}$  (within a 131k-token inference budget,  $4\times$  the 32k-token budget in the pretraining phase), with steady gains across domains (Figure 1c; Table 2). While our model can improve accuracy over 15% from 8 to 512 shots, vanilla LLMs exhibit limited scaling: o3-mini improves by only  $\sim 1.8\%$  (and even *declines* from 64 to 512 shots), while GPT-5-mini gains merely  $\sim 4.7\%$ . This indicates substantially higher sample efficiency of our approach.

### 3.2.3 MArCHINELEARNINGLM VS. TABULA-8B

Thanks to the *token-efficient prompting*, MArCHINELEARNINGLM supports an order of magnitude more demonstrations per prompt than TabuLa-8B (Table 3), which is typically capped by an 8k context (often  $\leq 20\text{--}32$  shots). In contrast, we scale stably to **1,024** shots for most tasks while *maintaining* significant many-shot gains, as shown in Appendix B. In the few-shot regime (e.g., 32-shot), MArCHINELEARNINGLM also outperforms TabuLa-8B on average—even though TabuLa explicitly exploits feature names—with particularly large gaps on certain datasets (e.g., a  $\sim 14.5\%$  shortfall for *vehicle* reported by TabuLa).

### 3.2.4 COMPETITIVE MANY-SHOT PERFORMANCE VS. STATE-OF-THE-ART TABULAR-SPECIFIC METHODS

Without any task-specific training, MArCHINELEARNINGLM reaches *random-forest-level* accuracy across  $M=8\text{--}512$  shots—typically within **2%** *relative* (Table 2)—and, even at 512 shots, outperforms random forest on roughly **30%** of tasks (Table 3). It also *clearly* surpasses simple instance-based learners (e.g., kNN) by **>4%** *relative* on average, indicating robust numerical modeling (Table 2; Table 3).

### 3.2.5 MArCHINELEARNINGLM VS. TABULAR ICL MODELS (TABICL / TABPFN)

As Table 2 shows, compared to state-of-the-art tabular ICL models like TabICL, MArCHINELEARNINGLM can be modestly behind at very high shot counts—largely due to LLM compute requirements. Unlike tabular architectures with row/column attention and specialized tokenizer (Hollmann et al.; Qu et al., 2025; Su et al., 2024; Wang et al., 2021), MArCHINELEARNINGLM uses a *general-purpose* LLM backbone yet remains *order-robust*: permuting in-prompt demonstrations leaves performance unchanged on average. Importantly, our method is *LLM-compatible* by design and thus uniquely positioned to exploit *external knowledge*, *heterogeneous/multimodal inputs*, and *reasoning-style* alignment (e.g., CoT), offering a practical path to close the remaining gap while retaining broad capabilities.

Table 3: Per-task test accuracy (%) with  $M \in \{32, 512\}$  shots. Abbreviations: Tabula = TabuLa-8B; Qwen = Qwen-2.5-7B-Instruct; Ours = MACHINELEARNINGLM (base: Qwen-2.5-7B-Instruct). To reduce memorization risks (Bordt et al.), all methods drop feature names/descriptions and encode only values except for TabuLa-8B, because we adopt the paper’s results on the overlapping datasets, using the setting that keeps the original header names. “EL” indicates the prompt exceeds TabuLa-8B’s token limit; “NA” indicates the dataset is not included in TabuLa-8B’s evaluation set.

Task	# Shots	KNN	RF	TabICL	Tabula	GPT-5-mini	o3-mini	Qwen	Ours
Bank	32	87.3	87.6	88.3	84.4	85.4	85.3	87.2	87.3
Bank	512	87.6	89.0	89.4	EL	87.8	86.7	88.1	88.7
BLE_RSSI_Indoor_Loc.	32	33.7	61.5	61.7	NA	59.4	61.2	44.7	63.7
BLE_RSSI_Indoor_Loc.	512	35.1	69.2	73.5	EL	61.4	58.4	52.7	70.3
Churn	32	84.6	86.5	86.6	91.4	82.1	79.1	85.4	86.7
Churn	512	86.6	91.1	92.0	EL	86.1	83.6	86.2	89.5
CMC	32	45.1	45.8	46.1	35.2	42.7	41.4	37.6	44.1
CMC	512	52.2	50.8	55.6	EL	41.0	42.7	50.2	50.2
Contaminant_10_0GHz	32	69.4	72.5	73.3	NA	60.8	53.3	55.6	71.7
Contaminant_10_0GHz	512	78.8	85.6	92.1	EL	60.4	49.4	62.7	82.3
Contaminant_9_5GHz	32	71.9	71.0	71.0	NA	55.0	53.8	53.5	73.8
Contaminant_9_5GHz	512	79.4	84.6	89.2	EL	53.1	48.5	59.4	80.4
Credit_g	32	64.0	69.0	72.0	70.3	70.0	63.5	58.5	71.5
Credit_g	512	70.0	76.0	76.5	EL	71.5	68.0	71.0	71.5
FICO_HELOC_Cleaned	32	59.0	64.7	68.3	NA	54.6	57.6	54.0	63.1
FICO_HELOC_Cleaned	512	64.3	71.5	71.3	EL	54.7	52.6	52.6	69.0
FOREX_AUDCHF_Day	32	50.7	52.3	51.2	EL	48.8	47.9	49.9	51.2
FOREX_AUDCHF_Day	512	44.4	52.6	71.1	EL	51.2	49.0	54.5	49.6
FOREX_AUDJPY_Day	32	45.5	46.6	49.0	NA	46.6	46.3	45.8	46.9
FOREX_AUDJPY_Day	512	57.8	61.3	72.8	EL	54.2	47.4	49.3	62.4
GAMETES_Heterog.	32	47.5	51.3	46.3	NA	52.2	48.8	48.1	49.1
GAMETES_Heterog.	512	57.8	59.7	71.3	EL	52.2	49.1	49.7	52.2
HELOC	32	59.8	66.0	58.7	EL	49.5	51.8	52.1	62.5
HELOC	512	65.6	71.3	72.3	EL	51.4	51.0	53.0	70.8
KC1	32	81.8	79.9	78.4	82.0	78.9	75.8	81.8	78.4
KC1	512	82.5	82.7	84.4	EL	81.9	78.7	83.4	83.9
LED24	32	30.8	41.9	46.4	NA	8.3	14.5	13.1	15.3
LED24	512	55.8	69.4	71.7	EL	9.1	12.3	11.7	48.4
LED7	32	55.9	57.7	58.8	EL	55.9	55.5	32.8	58.4
LED7	512	68.8	68.8	70.3	EL	66.6	57.3	48.4	66.9
Maternal_Health_Risk	32	45.8	52.7	60.1	NA	41.4	52.7	45.3	50.7
Maternal_Health_Risk	512	74.4	78.3	80.0	EL	73.9	63.0	59.6	78.3
PC1	32	92.3	92.3	90.1	89.8	88.7	88.3	85.1	88.7
PC1	512	91.9	93.7	94.1	EL	93.3	89.2	93.2	93.2
Phoneme	32	74.4	75.3	79.9	73.4	71.5	71.9	67.0	73.5
Phoneme	512	83.0	84.9	84.6	EL	69.6	64.3	68.7	82.0
Pima_Indians_Diabetes	32	64.9	74.7	66.9	70.3	69.5	61.0	65.6	71.4
Pima_Indians_Diabetes	512	68.8	75.3	74.7	EL	62.3	68.2	70.8	75.3
RingNorm	32	53.8	79.6	84.2	NA	66.2	75.9	69.2	93.2
RingNorm	512	58.6	93.5	97.0	EL	74.5	75.3	69.3	96.0
RL	32	56.6	58.5	55.8	NA	53.5	51.8	53.9	57.1
RL	512	60.7	66.7	68.5	EL	52.7	54.8	51.8	64.1
Segment	32	63.6	68.2	61.0	EL	60.4	51.5	32.0	64.7
Segment	512	88.1	90.9	93.5	EL	68.6	52.0	52.2	87.2
Seismic_Bumps	32	93.2	92.7	93.0	NA	91.3	86.3	92.5	90.3
Seismic_Bumps	512	92.8	92.8	93.0	EL	90.7	86.5	93.0	90.7
Statlog	32	61.0	65.0	64.0	NA	60.0	61.0	57.5	63.0
Statlog	512	67.0	74.0	72.5	EL	58.0	63.0	63.0	67.0
Thyroid	32	92.6	92.8	93.3	NA	92.3	91.2	92.6	92.8
Thyroid	512	94.0	98.0	98.8	EL	92.6	92.5	92.6	95.0
TwoNorm	32	94.4	88.8	95.9	NA	88.2	96.0	62.9	95.0
TwoNorm	512	97.0	95.9	97.6	EL	87.6	93.1	74.9	97.5
Vehicle	32	52.3	60.0	70.0	48.4	47.1	24.7	32.9	62.9
Vehicle	512	64.7	74.7	84.7	EL	41.2	27.1	32.4	72.9
WallRobot_Navigation	32	51.4	74.2	70.1	NA	43.0	35.8	42.0	60.1
WallRobot_Navigation	512	73.4	96.7	94.1	EL	48.9	35.8	45.2	83.3
Waveform	32	74.1	72.7	76.0	NA	44.2	40.5	38.6	72.5
Waveform	512	81.6	82.7	85.1	EL	32.4	33.0	43.5	84.0
Wine	32	63.8	64.6	68.7	NA	61.6	64.6	52.0	64.8
Wine	512	65.6	69.7	75.3	EL	56.2	56.4	56.2	71.0
Yeast	32	43.1	41.8	41.8	NA	36.7	40.4	33.7	41.8
Yeast	512	55.6	58.2	59.9	EL	42.8	36.7	32.3	59.3

Table 4: MMLU results for MACHINELEARNINGLM and baselines. (a) Macro accuracy across  $M$ -shot; (b) per-subject accuracies at 50-shot.

Number of shots	Qwen-2.5-7B-Instruct	Qwen-2.5-7B	TabuLa-8B	MACHINELEARNINGLM
0	73.8	73.5	61.6	73.2
10	75.9	75.5	65.2	75.1
50	75.8	75.4	N/A	75.4

(a) Macro accuracy on the full MMLU benchmark across different  $k$ -shot settings at  $temperature=0$ . TabuLa-8B (Gardner et al., 2024) uses a maximum 8k-token length.

(b) Per-subject accuracies at 50-shot.

Subject	Qwen-2.5-7B-Inst.	Qwen-2.5-7B	TabuLa-8B	MACHINELEARNINGLM
high_school_statistics	73.6	69.9	59.3	74.1
high_school_physics	62.9	55.6	47.7	61.6
astronomy	86.8	86.2	68.4	85.5
college_math	47.0	54.0	32.0	49.0
college_physics	53.9	61.8	53.9	57.8
conceptual_physics	74.0	74.0	62.1	76.2
econometrics	69.3	64.9	49.1	65.8
elementary_math	72.8	74.1	42.9	71.4
high_school_math	55.6	56.3	32.6	55.2

All accuracies (%) are reported using 50 shots, except for TabuLa-8B, which suggests a maximum sequence length of 8k and therefore uses a 20-shot setting. Models are evaluated with  $temperature=0.05$ ,  $\text{votes}=3$ .

### 3.2.6 MACHINELEARNINGLM IN GENERAL CHAT WORKFLOWS

As shown in Table 4, general abilities are *well preserved*. On MMLU, our model achieves  $\sim 73.2\%$  (0-shot) and  $\sim 75.4\%$  (50-shot), comparable to strong general-purpose LLMs. Notably, we observe consistent gains in numeracy-heavy subjects (e.g., high-school statistics/conceptual physics). Although training LLMs on real tables, TabuLa-8B underperforms on MMLU (by  $\sim 10\%$ ), underscoring that our training strategy of reusing the model architecture and tokenizer integrates smoothly with general LLM capabilities and remains compatible with future multimodal/heterogeneous extensions.

## 3.3 EMPIRICAL STUDY

**Numeric-dominant tables.** On pure numeric tables (e.g., `churn`, `maternal_health_risk`, `waveform`, `twonorm`, `vehicle`, `yeast`, `heloc`), our model remains competitive, indicating that the same prompt design handles both modalities without architecture changes.

**Heterogeneous (text+numeric) tables.** Our tabular encoding natively mixes free-text/categorical fields with numbers—*without* mandatory text bucketing or learned text embeddings—yielding reliable gains on heterogeneous schemas. On mixed-feature datasets such as `bank`, `adult`, `credit-g`, `online_shoppers`, `Bank_Customer_Churn_Dataset`, and `okcupid_stem`, MACHINELEARNINGLM consistently outperforms vanilla LLMs. *By contrast*, for highly symbolic/abstract textual fields that behave more like token sequences than NL (e.g., DNA base strings in the UCI `splice` dataset), MACHINELEARNINGLM falls short relative to numerical modeling methods such as Random Forests.

**High-cardinality labels.** On tasks with many classes (e.g., `kropt`, `letter` (26-way), `walking_activity`), MACHINELEARNINGLM underperforms strong tabular baselines (RF/TabICL). We attribute this to pretraining that sampled tasks with  $K \leq 10$  classes, biasing the decoder toward small label vocabularies; when  $K > 10$ , labels may become multi-token (e.g., “12”). Expanding  $K$  in synthesis is a promising mitigation.

**Resilience to class imbalance.** Across the task suite, MACHINELEARNINGLM remains stable under skewed label distributions: its many-shot accuracy tracks Random-Forest-level perfor-

mance while avoiding collapse-to-majority. On notably imbalanced datasets—e.g., `bank`, `pc1`, and `kc1`—it sustains competitive accuracy.

**Limits on forecasting-style tasks.** On time-series/forecasting tasks—particularly the FOREX variants (FOREX task series)—we observe significant declines relative to tabular methods. This gap is expected: our pretraining targets i.i.d. tabular prediction, whereas forecasting requires temporal inductive bias (lagged context, trend/seasonality priors) and higher numeric precision. We view this as an opportunity: future work will incorporate a time-aware strategy to better align MACHINELEARNINGLM with forecasting workloads. More limitations are detailed in Section 5.

## 4 RELATED WORK

**Many-shot ICL and scaling laws.** A growing literature observes that simply adding more demonstrations often yields diminishing or even negative returns in LLMs—e.g., one or a few high-quality demonstrations capture most gains (Chen et al.; Min et al., 2022; Liu et al., 2022; Pan, 2023), long-context usage is position-sensitive such as “lost in the middle” (Liu et al., 2024a; An et al.; Xiong et al., 2024), and many-shot gains can plateau in multimodal VLMs such as Flamingo beyond  $\sim 32$  shots (Alayrac et al., 2022; Tai et al., 2024). Recent efforts improve many-shot ICL via specialized training or mechanisms: DeepMind’s study shows task-dependent trends and proposes reinforced/unsupervised ICL variants (Agarwal et al., 2024) to mitigate many-shot scaling; DrICL reweights demonstrations and modifies objectives to mitigate plateauing (Zhang et al., 2025); semi-supervised many-shot ICL mitigates many-shot scaling when using self-generated annotations (Gu et al.); multimodal works report mixed but often dataset-specific monotonic gains with longer contexts (Jiang et al.). Moreover, long-context evaluation disentangles retrieval-like tasks from global context understanding, with many models degrading on the latter at 16k tokens (Zou et al., 2025). TabDPT reports scaling laws with respect to both model size and pretraining-corpus size Ma et al. (2024). Unlike these approaches, MACHINELEARNINGLM induces many-shot ICL *through pre-training on millions of synthetic tabular tasks*, yielding *monotonic example-count scaling* while preserving the general reasoning of the base LLM.

**LM-based ML learner.** Compared with TabLLM (Hegselmann et al., 2023)—an approach that demands computationally intensive, task-specific fine-tuning and hyper-parameter tuning—MACHINELEARNINGLM adapts to new tabular tasks *purely* through ICL at inference time, with no gradient updates. Crucially, it delivers markedly stronger reasoning over large volumes of numerical data, a long-standing weakness of TabLLM<sup>6</sup>. Most relevant to us, (Gardner et al., 2024) proposes TabuLa-8B—finetuning Llama 3-8B on a web-scale corpus (T4) distilled from TabLib, and introducing a row-causal tabular masking (RCTM) scheme that packs samples by table and encourages few-shot behavior (Gardner et al., 2024). Their main evaluations focus on  $k \in [0, 32]$  shots. Our synthetic pretraining complements real-world data pretraining and differs in three ways: (i) we *continue pretraining* a general-purpose LLM *without architectural modifications* without losing the backbone’s general capabilities, (ii) we pretrain on *synthetic, SCM-driven* tabular tasks with explicitly controlled diversity, ensuring no dataset leakage from downstream evaluations, and (iii) we target *many-shot ICL* behavior on tabular tasks (1,024 demonstrations under a fixed context budget) using our proposed token-efficient method.

**In-context tabular ML learners.** TabPFN frames tabular classification as ICL with a pre-trained transformer hypernetwork and achieves strong few-shot accuracy on small tables (Hollmann et al.). TabICL scales PFN-style ICL to much larger tables via a two-stage, column-then-row architecture and synthetic pretraining (Qu et al., 2025). However, these tabular ICL models are trained independently of language models—incompatible with LM architectures or checkpoints—so they lack general text reasoning and open-domain knowledge, which limits application when textual fields carry meaning and constrains performance on multimodal (text–numeric) tasks. In contrast, MACHINELEARNINGLM is built upon a pre-trained LLM backbone and therefore combines robust numeric processing with the ability to interpret textual headers, free-text cells, and world knowledge priors, offering a unified foundation model for heterogeneous, real-world in-context ML tasks.

<sup>6</sup><https://gael-varoquaux.info/science/carte-toward-table-foundation-models.html>

**Tool-using agents for ML vs. in-context learners.** A complementary line of work evaluates or builds LLM agents that *call external ML toolchains* (e.g., LightGBM/XGBoost/CatBoost, AutoML) to solve end-to-end ML engineering tasks, as in MLE-Bench (Chan et al., 2024), MLAGent-Bench (Huang et al., 2024), R&D-Agent (Yang et al., 2025), and ML-Master (Anonymous, 2025). However, their performance is bound by the invoked learners and pipelines. In contrast, MACHINE-LEARNINGLM explores a way to *internalize* the learning procedure: the model performs in-context prediction, requiring neither per-task fine-tuning nor calls to external ML models, and MACHINE-LEARNINGLM can also be called by the MLE agent as a tool.

## 5 LIMITATIONS

While MACHINELEARNINGLM shows strong in-context ML performance, several limitations remain.

- **Task scope.** Our pretraining corpus focuses on *tabular classification* synthesized from SCMs. We do not yet cover regression, ranking, time-series forecasting, or structured prediction, and we cap the number of classes ( $K \leq 10$ ). Extending beyond IID rows (e.g., temporal or relational dependencies) is future work.
- **Context length and compute.** Continued pretraining used a 32k-token context; although inference generalizes beyond this (tested up to  $\sim 131$ k tokens), scaling to many thousands of shots like TabPFN/TabICL remains challenging due to compute and memory costs.
- **Numerical encoding trade-offs.** The  $[0, 999]$  integer mapping preserves order but *coarsens* magnitudes and can obscure semantically meaningful constants (e.g., age 18). As context windows grow, more expressive number encodings can be explored to retain such cues while remaining token-efficient.
- **Warm-start bias.** The RF-mimic warm-up and example-level consensus filtering may bias early training toward tree-like decision boundaries and easy examples. Although we disable consensus after warm-up, some inductive bias may persist; we currently distill *labels only* (not rationales). How to best leverage external teachers is still an open question.
- **Model scale and adaptation.** Results are with a 7B backbone and low-rank adaptation (LoRA rank 8). Larger backbones, alternative adapters, or optimizer/regularization choices may further improve many-shot numeracy but were not explored here.

## 6 FUTURE WORK

We hope MACHINELEARNINGLM will ignite new lines of research, as exemplified below. Feel free to contact us for further discussions .

- **Beyond text and numbers: synthetic tasks with multimodal features.** Starting from our synthetic tabular tasks, map numerical/categorical features to *weakly labeled* multimodal surrogates—short texts, speech snippets, images, geospatial signals, or time series—using generative back-ends (LLM/VLM/TTS) conditioned on latent factors to preserve coarse class semantics. This produces controllable, cross-modal pairs aligned with the tabular schema<sup>7</sup> and enables MACHINELEARNINGLM to practice multimodal in-context prediction on heterogeneous signals.
- **Longer contexts via parallelism and system optimizations.** Extend context length using tensor/pipeline parallelism and memory-efficient attention/KV caching to support substantially more in-prompt examples. Recent work on cache-augmented architectures demonstrates that principled KV-cache management can significantly improve efficiency and scalability for long-context reasoning (Bhaskar et al., 2025), suggesting promising directions to integrate such mechanisms into MACHINELEARNINGLM.
- **Toward interpretability: narrative distillation and reasoning-augmented learning.** Each task in our pretraining corpus is generated from a structural causal model (SCM),

<sup>7</sup>Table formats (e.g., HTML tables) naturally organize images, hyperlinks, and embedded objects.

which we treat as an intrinsic source of explanation. We train the LM to *narrate* the underlying SCM—variables, relations, and mechanisms—as an auxiliary objective aligned with the prediction task, thereby yielding more faithful rationales and stronger reasoning. Moreover, couple feature attribution signals (e.g., SHAP (Lundberg & Lee, 2017) / LIME (Ribeiro et al., 2016)) with MACHINELEARNINGLM’s generation to produce faithful instance- and cohort-level narratives, while distilling rules from ensembles (e.g., in-Trees (Deng, 2014) / RuleFit (Friedman & Popescu, 2008)) into compact, human-readable reasoning traces. Recent advances such as DeepSeek-R1 (Guo et al., 2025) demonstrate the promise of incentivizing reasoning capability in LLMs through RL. This integration promises not only accurate predictions but also transparent rationales, enhancing compliance and trust.

- **Uncertainty-aware responses.** Recent analyses from OpenAI argue that training/evaluation schemes which *penalize* uncertainty and implicitly *reward* guessing are a root cause of hallucinations<sup>8</sup>. We suspect a similar incentive mismatch in our setting. Future work may (i) train on *teacher predictive distributions*—e.g., randomized/ensemble teachers that provide calibrated confidences—instead of hard labels, optimized with proper scoring rules (NLL/Brier) and selective-prediction losses that allow abstention; (ii) explicitly represent and reward well-calibrated uncertainty in the output schema (e.g., an UNCERTAIN/defer option with risk-coverage evaluation); and (iii) directly optimize task-level metrics (AU-ROC, RMSE, F1) via reinforcement learning or differentiable surrogates, with robust reward shaping (e.g., clipped/Huberized or quantile-based rewards) to reduce outlier sensitivity and improve end-to-end utility.
- **Combined with Retrieval-Augmented Methods.** Retrieval-augmented method has shown that attaching a retrieval module to LLMs enables scalable any-shot learning and yields power-law error reductions as data grows (Wen et al., 2025). Integrating such retrieval into MACHINELEARNINGLM can boost many-shot example limits by dynamically injecting the most relevant examples during pretraining and inference.
- **Real-data alignment via continued fine-tuning.** Beyond purely synthetic pretraining, we will perform lightweight continued fine-tuning on a curated suite of real tabular prediction tasks to better align with practical distributions.
- **Extending MACHINELEARNINGLM to fully leverage Agent Memory.** Recent advances leverage memory mechanisms so that agents can recall and reuse successful or similar past experiences to inform their next action (Wang et al., 2023; Lin et al., 2025; Wang et al., b). Such experiences may be textual traces, numerical features, or temporal signals. By pretraining the policy model with many-shot in-context experiences, the agent can improve decision-making and robustness in dynamic environments.
- **Integration with MLE agents.** Fuse MACHINELEARNINGLM with MLE-agent-style planners to orchestrate end-to-end MLE workflows. The agent treats MACHINELEARNINGLM both as a solver and as an internal tool, enabling a flexible interface with heterogeneous real-world MLE tasks.

## 7 CONCLUSION

We introduced MACHINELEARNINGLM, a portable continued-pretraining recipe that equips a general-purpose LLM with robust in-context tabular prediction *without* architectural or tokenizer changes. By synthesizing millions of SCM-driven tasks and using a Random-Forest warm start, the model acquires strong numerical modeling while preserving general knowledge and reasoning. A token-efficient tabular encoding, integer-based number normalization, and sequence-level batch-prediction together expand the effective context budget and amortize prompt overhead. Across diverse out-of-distribution classification tasks, MACHINELEARNINGLM remarkably improves over its backbone and approaches random-forest-level accuracy from 8 to 512 shots; accuracy further increases up to 1,024 shots and is robust to exemplar-order permutations. These results indicate that targeted continued pretraining on synthetic prediction tasks is a practical path to scaling many-shot ICL within general-purpose LLMs. Finally, we discuss the current limitations and chart several promising avenues for future work.

<sup>8</sup><https://openai.com/index/why-language-models-hallucinate/>

## AUTHOR CONTRIBUTIONS

**Conceptualization** (*LLM continued pretraining with SCM-based synthesis, RF-mimic warm-start, token-efficient prompting, and order-robust self-consistency*): Haoyu Dong<sup>9</sup>.

**Methodology**: Pretraining recipe and objectives — Haoyu Dong, Pengkun Zhang<sup>10</sup>; SCM task synthesis — Pengkun Zhang, Haoyu Dong; RF-mimic warm-start (gating and consensus filtering) — Haoyu Dong; token-efficient prompting — Haoyu Dong; self-consistency — Yanzhen Shen<sup>11</sup>, Mingzhe Lu<sup>12</sup>, Haoyu Dong.

**Software & Engineering**: Pretraining pipeline and training scripts — Pengkun Zhang, Haoyu Dong; evaluation harness — Yanzhen Shen, Mingzhe Lu, Haoyu Dong; SCM generator and data pipelines — Pengkun Zhang, Haoyu Dong; token-efficient prompting utilities — Haoyu Dong; code optimization, cross-platform support, and parallelization — Mingzhe Lu, Pengkun Zhang.

**Investigation & Validation**: Experiments and statistical aggregation of results — Mingzhe Lu, Pengkun Zhang, Haoyu Dong.

**Writing**: Original draft (*main text, tables, and figures*) — Haoyu Dong; review and editing — Yanzhen Shen, Pengkun Zhang, Mingzhe Lu, Guolin Ke<sup>13</sup>.

**Limitations & Future Work**: Haoyu Dong, Guolin Ke.

**ML Expertise**: High-level guidance on ML practice, interpretability, and online/continual learning directions — Guolin Ke.

Moreover, we thank Hui Xue for suggestions on method and evaluation, including adding the MMLU benchmark and future directions that leverage random-forest predictive probabilities.

## REFERENCES

- Rishabh Agarwal, Avi Singh, Lei Zhang, Bernd Bohnet, Luis Rosias, Stephanie Chan, Biao Zhang, Ankesh Anand, Zaheer Abbas, Azade Nova, et al. Many-shot in-context learning. *Advances in Neural Information Processing Systems*, 37:76930–76966, 2024.
- Jean-Baptiste Alayrac, Jeff Donahue, Pauline Luc, Antoine Miech, Iain Barr, Yana Hasson, Karel Lenc, Arthur Mensch, Katherine Millican, Malcolm Reynolds, et al. Flamingo: a visual language model for few-shot learning. *Advances in neural information processing systems*, 35:23716–23736, 2022.
- Chenxin An, Jun Zhang, Ming Zhong, Lei Li, Shansan Gong, Yao Luo, Jingjing Xu, and Lingpeng Kong. Why does the effective context length of llms fall short? In *The Thirteenth International Conference on Learning Representations*.
- Anonymous. MI-master: Towards ai-for-ai via integration of exploration and reasoning. *arXiv preprint arXiv:2506.16499*, 2025. URL <https://arxiv.org/abs/2506.16499>.
- Jinze Bai, Shuai Bai, Yunfei Chu, Zeyu Cui, Kai Dang, Xiaodong Deng, Yang Fan, Wenbin Ge, Yu Han, Fei Huang, et al. Qwen technical report. *arXiv preprint arXiv:2309.16609*, 2023.
- Adithya Bhaskar, Alexander Wettig, Tianyu Gao, Yihe Dong, and Danqi Chen. Cache me if you can: How many kvs do you need for effective long-context lms? *arXiv preprint arXiv:2506.17121*, 2025.
- Sebastian Bordt, Harsha Nori, Vanessa Cristina Rodrigues Vasconcelos, Besmira Nushi, and Rich Caruana. Elephants never forget: Memorization and learning of tabular data in large language models. In *First Conference on Language Modeling*.
- 
- <sup>9</sup>University of Chinese Academy of Sciences, donghaoyu22@mails.ucas.edu.cn
- <sup>10</sup>South China University of Technology, sezhengpengkun@mail.scut.edu.cn
- <sup>11</sup>Stanford University, yanzhen4@stanford.edu
- <sup>12</sup>University of Chinese Academy of Sciences, lumingzhe23@mails.ucas.edu.cn
- <sup>13</sup>Individual, guolin.ke@outlook.com

- Leo Breiman. Random forests. *Machine Learning*, 45(1):5–32, 2001.
- Tom Brown, Benjamin Mann, Nick Ryder, Melanie Subbiah, Jared D Kaplan, Prafulla Dhariwal, Arvind Neelakantan, Pranav Shyam, Girish Sastry, Amanda Askell, et al. Language models are few-shot learners. *Advances in neural information processing systems*, 33:1877–1901, 2020.
- Jun Shern Chan et al. Mle-bench: Evaluating machine learning agents on real-world competitions. *arXiv preprint arXiv:2410.07095*, 2024. URL <https://arxiv.org/abs/2410.07095>.
- Jiuhai Chen, Lichang Chen, Chen Zhu, and Tianyi Zhou. How many demonstrations do you need for in-context learning? In *The 2023 Conference on Empirical Methods in Natural Language Processing*.
- Tianqi Chen and Carlos Guestrin. Xgboost: A scalable tree boosting system. In *KDD*, pp. 785–794, 2016.
- Zhoujun Cheng, Jungo Kasai, and Tao Yu. Batch prompting: Efficient inference with large language model apis. In *Proceedings of the 2023 Conference on Empirical Methods in Natural Language Processing: Industry Track*, pp. 792–810, 2023.
- Hyung Won Chung, Le Hou, Shayne Longpre, Barret Zoph, Yi Tay, William Fedus, Yunxuan Li, Xuezhi Wang, Mostafa Dehghani, Siddhartha Brahma, et al. Scaling instruction-finetuned language models. *Journal of Machine Learning Research*, 25(70):1–53, 2024.
- Thomas M. Cover and Peter E. Hart. Nearest neighbor pattern classification. *IEEE Transactions on Information Theory*, 13(1):21–27, 1967.
- Houtao Deng. Interpreting tree ensembles with intrees. *arXiv preprint arXiv:1408.5456*, 2014.
- Haoyu Dong, Jianbo Zhao, Yuzhang Tian, Junyu Xiong, Shiyu Xia, Mengyu Zhou, Yun Lin, José Cambronero, Yeye He, Shi Han, et al. Spreadsheetlm: encoding spreadsheets for large language models. In *Proceedings of the 2024 Conference on Empirical Methods in Natural Language Processing*, pp. 20728–20748, 2024.
- Yu Fei, Yifan Hou, Zeming Chen, and Antoine Bosselut. Mitigating label biases for in-context learning. In *The 61st Annual Meeting Of The Association For Computational Linguistics*, 2023.
- Jerome H. Friedman and Bogdan E. Popescu. Predictive learning via rule ensembles. *The Annals of Applied Statistics*, 2(3):916–954, 2008. doi: 10.1214/07-AOAS148.
- Josh Gardner, Juan C Perdomo, and Ludwig Schmidt. Large scale transfer learning for tabular data via language modeling. *Advances in Neural Information Processing Systems*, 37:45155–45205, 2024.
- Zhengyao Gu, Henry Peng Zou, Aiwei Liu, Yankai Chen, Weizhi Zhang, and Philip S Yu. Scaling laws for many-shot in-context learning with self-generated annotations. In *ICML 2025 Workshop on Long-Context Foundation Models*.
- Daya Guo, Dejian Yang, Haowei Zhang, Junxiao Song, Ruoyu Zhang, Runxin Xu, Qihao Zhu, Shirong Ma, Peiyi Wang, Xiao Bi, et al. Deepseek-r1: Incentivizing reasoning capability in llms via reinforcement learning. *arXiv preprint arXiv:2501.12948*, 2025.
- Stefan Hegselmann, Alejandro Buendia, Hunter Lang, Monica Agrawal, Xiaoyi Jiang, and David Sontag. Tabllm: Few-shot classification of tabular data with large language models. In *International conference on artificial intelligence and statistics*, pp. 5549–5581. PMLR, 2023.
- Geoffrey Hinton, Oriol Vinyals, and Jeff Dean. Distilling the knowledge in a neural network. *arXiv preprint arXiv:1503.02531*, 2015.
- Noah Hollmann, Samuel Müller, Katharina Eggensperger, and Frank Hutter. Tabpfn: A transformer that solves small tabular classification problems in a second. In *The Eleventh International Conference on Learning Representations*.

- Noah Hollmann, Samuel Müller, Lennart Purucker, Arjun Krishnakumar, Max Körfer, Shi Bin Hoo, Robin Tibor Schirrmeister, and Frank Hutter. Accurate predictions on small data with a tabular foundation model. *Nature*, 637(8045):319–326, 2025.
- Edward J Hu, Yelong Shen, Phillip Wallis, Zeyuan Allen-Zhu, Yuanzhi Li, Shean Wang, Lu Wang, Weizhu Chen, et al. Lora: Low-rank adaptation of large language models. *ICLR*, 1(2):3, 2022.
- Qian Huang, Jian Vora, Percy Liang, and Jure Leskovec. Mlagentbench: evaluating language agents on machine learning experimentation. In *Proceedings of the 41st International Conference on Machine Learning*, pp. 20271–20309, 2024.
- Hugging Face. Number tokenization blog, 2024. URL <https://huggingface.co/spaces/huggingface/number-tokenization-blog>. Hugging Face Spaces; last updated Nov 29, 2024.
- Yixing Jiang, Jeremy Andrew Irvin, Ji Hun Wang, Muhammad Ahmed Chaudhry, Jonathan H Chen, and Andrew Y Ng. Many-shot in-context learning in multimodal foundation models. In *ICML 2024 Workshop on In-Context Learning*.
- Guolin Ke, Qi Meng, Thomas Finley, Taifeng Wang, Wei Chen, Weidong Ma, Qiwei Ye, and Tie-Yan Liu. Lightgbm: A highly efficient gradient boosting decision tree. In *NeurIPS*, 2017.
- Diederik P Kingma and Jimmy Ba. Adam: A method for stochastic optimization. *arXiv preprint arXiv:1412.6980*, 2014.
- Jianzhe Lin, Maurice Diesendruck, Liang Du, and Robin Abraham. Batchprompt: Accomplish more with less. In *The Twelfth International Conference on Learning Representations*.
- Jiaye Lin, Yifu Guo, Yuzhen Han, Sen Hu, Ziyi Ni, Licheng Wang, Mingguang Chen, Dixin Jiang, Binxing Jiao, Chen Hu, et al. Se-agent: Self-evolution trajectory optimization in multi-step reasoning with llm-based agents. *arXiv preprint arXiv:2508.02085*, 2025.
- Nick Littlestone and Manfred K Warmuth. The weighted majority algorithm. *Information and computation*, 108(2):212–261, 1994.
- Jiachang Liu, Dinghan Shen, Yizhe Zhang, William B Dolan, Lawrence Carin, and Weizhu Chen. What makes good in-context examples for gpt-3? In *Proceedings of Deep Learning Inside Out (DeeLIO 2022): The 3rd Workshop on Knowledge Extraction and Integration for Deep Learning Architectures*, pp. 100–114, 2022.
- Nelson F Liu, Kevin Lin, John Hewitt, Ashwin Paranjape, Michele Bevilacqua, Fabio Petroni, and Percy Liang. Lost in the middle: How language models use long contexts. *Transactions of the Association for Computational Linguistics*, 11:157–173, 2024a.
- Si-Yang Liu, Hao-Run Cai, Qi-Le Zhou, and Han-Jia Ye. Talent: A tabular analytics and learning toolbox. *arXiv preprint arXiv:2407.04057*, 2024b.
- Scott M Lundberg and Su-In Lee. A unified approach to interpreting model predictions. In *Advances in Neural Information Processing Systems (NeurIPS)*, volume 30, 2017.
- Junwei Ma, Valentin Thomas, Rasa Hosseinzadeh, Hamidreza Kamkari, Alex Labach, Jesse C Cresswell, Keyvan Golestan, Guangwei Yu, Maksims Volkovs, and Anthony L Caterini. Tab-dpt: Scaling tabular foundation models. *arXiv preprint arXiv:2410.18164*, 2024.
- Sewon Min, Xinxin Lyu, Ari Holtzman, Mikel Artetxe, Mike Lewis, Hannaneh Hajishirzi, and Luke Zettlemoyer. Rethinking the role of demonstrations: What makes in-context learning work? In Yoav Goldberg, Zornitsa Kozareva, and Yue Zhang (eds.), *Proceedings of the 2022 Conference on Empirical Methods in Natural Language Processing*, pp. 11048–11064, Abu Dhabi, United Arab Emirates, December 2022. Association for Computational Linguistics. doi: 10.18653/v1/2022.emnlp-main.759. URL <https://aclanthology.org/2022.emnlp-main.759/>.
- Martin Mráz, Breenda Das, Anshul Gupta, Lennart Purucker, and Frank Hutter. Towards benchmarking foundation models for tabular data with text. *arXiv preprint arXiv:2507.07829*, 2025.

- Mateusz Ochal, Massimiliano Patacchiola, Jose Vazquez, Amos Storkey, and Sen Wang. Few-shot learning with class imbalance. *IEEE Transactions on Artificial Intelligence*, 4(5):1348–1358, 2023.
- OpenAI. Openai changelog: o3-mini released. <https://platform.openai.com/docs/changelog>, 2024. Lists the o3-mini reasoning model.
- OpenAI. Openai o3 and o4-mini system card. <https://openai.com/systems/o3/>, 2025. System card covering the o3 family and o4-mini.
- Jane Pan. What in-context learning “learns” in-context: Disentangling task recognition and task learning. Master’s thesis, Princeton University, 2023.
- Judea Pearl. *Causality*. Cambridge university press, 2009.
- Jonas Peters, Dominik Janzing, and Bernhard Schölkopf. *Elements of causal inference: foundations and learning algorithms*. The MIT press, 2017.
- Liudmila Prokhorenkova, Gleb Gusev, Aleksandr Vorobev, Anna Veronika Dorogush, and Andrey Gulin. Catboost: Unbiased boosting with categorical features. In *Advances in Neural Information Processing Systems (NeurIPS)*, volume 31, 2018.
- Jingang Qu, David Holzmüller, Gaël Varoquaux, and Marine Le Morvan. Tabicl: A tabular foundation model for in-context learning on large data. In *ICML 2025-Forty-Second International Conference on Machine Learning*, 2025.
- Marco Tulio Ribeiro, Sameer Singh, and Carlos Guestrin. "why should i trust you?": Explaining the predictions of any classifier. In *Proceedings of the 22nd ACM SIGKDD International Conference on Knowledge Discovery and Data Mining (KDD)*, pp. 1135–1144, 2016.
- Xingjian Shi, Jonas Mueller, Nick Erickson, Mu Li, and Alexander J Smola. Benchmarking multimodal automl for tabular data with text fields. *arXiv preprint arXiv:2111.02705*, 2021.
- Noah Shinn, Federico Cassano, Ashwin Gopinath, Karthik Narasimhan, and Shunyu Yao. Reflexion: Language agents with verbal reinforcement learning. *Advances in Neural Information Processing Systems*, 36:8634–8652, 2023.
- Aaditya K Singh and DJ Strouse. Tokenization counts: the impact of tokenization on arithmetic in frontier llms. *arXiv preprint arXiv:2402.14903*, 2024.
- Georgios Spithourakis and Sebastian Riedel. Numeracy for language models: Evaluating and improving their ability to predict numbers. In *Proceedings of the 56th Annual Meeting of the Association for Computational Linguistics (Volume 1: Long Papers)*, pp. 2104–2115, 2018.
- Aofeng Su, Aowen Wang, Chao Ye, Chen Zhou, Ga Zhang, Gang Chen, Guangcheng Zhu, Haobo Wang, Haokai Xu, Hao Chen, et al. Tablegpt2: A large multimodal model with tabular data integration. *arXiv preprint arXiv:2411.02059*, 2024.
- Yuan Sui, Mengyu Zhou, Mingjie Zhou, Shi Han, and Dongmei Zhang. Table meets llm: Can large language models understand structured table data? a benchmark and empirical study. In *Proceedings of the 17th ACM International Conference on Web Search and Data Mining (WSDM)*, 2024. doi: 10.1145/3616855.3635752.
- Yan Tai, Weichen Fan, Zhao Zhang, Feng Zhu, Rui Zhao, and Ziwei Liu. Link-context learning for multimodal llms. In *Proceedings of the IEEE/CVF Conference on Computer Vision and Pattern Recognition (CVPR)*, 2024. URL [https://openaccess.thecvf.com/content/CVPR2024/papers/Tai\\_Link-Context\\_Learning\\_for\\_Multimodal\\_LLMS\\_CVPR\\_2024\\_paper.pdf](https://openaccess.thecvf.com/content/CVPR2024/papers/Tai_Link-Context_Learning_for_Multimodal_LLMS_CVPR_2024_paper.pdf).
- Eric Wallace, Yizhong Wang, Sujian Li, Sameer Singh, and Matt Gardner. Do NLP models know numbers? probing numeracy in embeddings. In *Proceedings of the 2019 Conference on Empirical Methods in Natural Language Processing and the 9th International Joint Conference on Natural Language Processing (EMNLP-IJCNLP)*, pp. 5307–5315, Hong Kong, China, November 2019. Association for Computational Linguistics. doi: 10.18653/v1/D19-1534. URL <https://aclanthology.org/D19-1534/>.

Guanzhi Wang, Yuqi Xie, Yunfan Jiang, Ajay Mandlekar, Chaowei Xiao, Yuke Zhu, Linxi Fan, and Anima Anandkumar. Voyager: An open-ended embodied agent with large language models. *arXiv preprint arXiv:2305.16291*, 2023.

Xuezhi Wang, Jason Wei, Dale Schuurmans, Quoc V Le, Ed H Chi, Sharan Narang, Aakanksha Chowdhery, and Denny Zhou. Self-consistency improves chain of thought reasoning in language models. In *The Eleventh International Conference on Learning Representations*, a.

Xuezhi Wang, Jason Wei, Dale Schuurmans, Quoc Le, Ed Chi, Sharan Narang, Aakanksha Chowdhery, and Denny Zhou. Self-consistency improves chain of thought reasoning in language models. *arXiv preprint arXiv:2203.11171*, 2022a.

Yizhong Wang, Swaroop Mishra, Pegah Alipoormolabashi, Yeganeh Kordi, Amirreza Mirzaei, Anjana Arunkumar, Arjun Ashok, Arut Selvan Dhanasekaran, Atharva Naik, David Stap, et al. Super-naturalinstructions: Generalization via declarative instructions on 1600+ nlp tasks. *arXiv preprint arXiv:2204.07705*, 2022b.

Zhiruo Wang, Haoyu Dong, Ran Jia, Jia Li, Zhiyi Fu, Shi Han, and Dongmei Zhang. Tuta: Tree-based transformers for generally structured table pre-training. In *Proceedings of the 27th ACM SIGKDD Conference on Knowledge Discovery & Data Mining*, pp. 1780–1790, 2021.

Zora Zhiruo Wang, Jiayuan Mao, Daniel Fried, and Graham Neubig. Agent workflow memory. In *Forty-second International Conference on Machine Learning*, b.

Xumeng Wen, Shun Zheng, Zhen Xu, Yiming Sun, and Jiang Bian. Scalable in-context learning on tabular data via retrieval-augmented large language models. *arXiv preprint arXiv:2502.03147*, 2025.

Wenhan Xiong, Jingyu Liu, Igor Molybog, Hejia Zhang, Prajjwal Bhargava, Rui Hou, Louis Martin, Rashi Rungta, Karthik Abinav Sankararaman, Barlas Oguz, et al. Effective long-context scaling of foundation models. In *Proceedings of the 2024 Conference of the North American Chapter of the Association for Computational Linguistics: Human Language Technologies (Volume 1: Long Papers)*, pp. 4643–4663, 2024.

Xu Yang, Xiao Yang, Shikai Fang, Bowen Xian, Yuante Li, Jian Wang, Minrui Xu, Haoran Pan, Xinpeng Hong, Weiqing Liu, et al. R&d-agent: Automating data-driven ai solution building through llm-powered automated research, development, and evolution. *arXiv preprint arXiv:2505.14738*, 2025.

Han-Jia Ye, Si-Yang Liu, Hao-Run Cai, Qi-Le Zhou, and De-Chuan Zhan. A closer look at deep learning methods on tabular datasets. *arXiv preprint arXiv:2407.00956*, 2024.

Xiaoqing Zhang, Ang Lv, Yuhan Liu, Flood Sung, Wei Liu, Jian Luan, Shuo Shang, Xiuying Chen, and Rui Yan. More is not always better? enhancing many-shot in-context learning with differentiated and reweighting objectives. In *Proceedings of ACL 2025 (Long Papers)*, 2025. URL <https://aclanthology.org/2025.acl-long.1475.pdf>.

Zihao Zhao, Eric Wallace, Shi Feng, Dan Klein, and Sameer Singh. Calibrate before use: Improving few-shot performance of language models. In *International conference on machine learning*, pp. 12697–12706. PMLR, 2021.

Yaowei Zheng, Richong Zhang, Junhao Zhang, Yanhan Ye, Zheyuan Luo, and Yongqiang Ma. Llamafactory: Unified efficient fine-tuning of 100+ language models, 2024. URL <https://arxiv.org/abs/2403.13372>.

Kaijian Zou, Muhammad Khalifa, and Lu Wang. On many-shot in-context learning for long-context evaluation. In Wanxiang Che, Joyce Nabende, Ekaterina Shutova, and Mohammad Taher Pilehvar (eds.), *Proceedings of the 63rd Annual Meeting of the Association for Computational Linguistics (Volume 1: Long Papers)*, pp. 25605–25639, Vienna, Austria, July 2025. Association for Computational Linguistics. ISBN 979-8-89176-251-0. doi: 10.18653/v1/2025.acl-long.1245. URL <https://aclanthology.org/2025.acl-long.1245/>.

## A LIST OF SYMBOLS

Symbol	Meaning	Range/Default
$\mathcal{G}$	DAG of the structural causal model (SCM)	—
$v$	Node index in $\mathcal{G}$	—
$x_v$	Variable value at node $v$	—
$f_v$	Structural function at node $v$	—
$\varepsilon_v$	i.i.d. noise term	—
$M$	# in-context demonstrations (shots)	$\leq 1024$
$N$	# query/test rows predicted per batched sequence	50
$d$	Feature dimension (columns)	$5 \sim 50$
$K$	# classes	$2 \sim 10$
$S$	Demonstration set $\{s_i\}_{i=1}^M$	—
$Q$	Query set $\{x^{(i)}\}_{i=1}^N$	—
$y$	Target JSON array of predictions	—
$\hat{\ell}_i$	Predicted label for query $i$	—
$\text{tok}(\cdot)$	Tokenizer	—
$T$	Target token length	—
$\theta$	Model parameters	—
$\mathcal{L}(\theta)$	Training loss (NLL)	—
$H$	Token cost of the instruction/schema header	—
$R$	Per-row token cost (demo or query)	—
$C$	Amortized token cost per predicted label	—
$z$	$z$ -score normalized numeric value	—
$i$	Integer after $[0, 999]$ -norm mapping	—
$p_0$	Conservative random baseline accuracy	—
$N_{\text{correct}}$	# correct predictions by RF per batched sequence	—
$\alpha$	One-sided binomial test threshold	0.2
$\kappa$	Cohen's $\kappa$ (chance-corrected agreement)	$> 0.01$
$\delta_{\text{bacc}}$	Balanced-accuracy margin	0.03
$\delta_{\text{F1}}$	Macro-F1 margin	0.00
$\tau_{\text{dom}}$	Max dominant-class fraction	0.95
$V$	# shuffled prompt variants	5
$p_i(y_j)$	Next-token prob. for label $y_j$ under variant $P_i$	—
$\tilde{p}(y_j)$	Aggregated prob.: $\sum_{i=0}^{V-1} p_i(y_j)$	—

## B MANY-SHOT SCALING PER-TASK EVALUATION

Table 6: Per-dataset test accuracy from 8 to 1,024 shots on more sampled domain-representative datasets in Talent. Abbreviations: Qwen-2.5-7B = Qwen-2.5-7B-Instruct; Our = MACHINE-LEARNINGLM (base: Qwen-2.5-7B-Instruct).

Dataset	Shots	KNN	RF	Qwen-2.5-7B	Our
bank	8	0.8657	0.8695	0.8526	0.8704
bank	16	0.8723	0.8759	0.8666	0.8707
bank	32	0.8725	0.8764	0.8722	0.8727
bank	64	0.8764	0.8828	0.8780	0.8771
bank	128	0.8778	0.8847	0.8798	0.8830
bank	256	0.8757	0.8873	0.8803	0.8867
bank	512	0.8762	0.8897	0.8808	0.8870
bank	1,024	0.8801	0.8947	0.8795	0.8903
BLE_RSSI_dataset_for_Indoor_localization	8	0.3385	0.5167	0.3956	0.5328
BLE_RSSI_dataset_for_Indoor_localization	16	0.3525	0.5884	0.4382	0.5889
BLE_RSSI_dataset_for_Indoor_localization	32	0.3370	0.6154	0.4467	0.6375
BLE_RSSI_dataset_for_Indoor_localization	64	0.3360	0.6560	0.4567	0.6715
BLE_RSSI_dataset_for_Indoor_localization	128	0.3400	0.6960	0.4852	0.6950
BLE_RSSI_dataset_for_Indoor_localization	256	0.3460	0.6865	0.5153	0.7020
BLE_RSSI_dataset_for_Indoor_localization	512	0.3515	0.6915	0.5268	0.7031
BLE_RSSI_dataset_for_Indoor_localization	1,024	0.3375	0.6955	0.5238	0.7126
churn	8	0.8260	0.8460	0.7970	0.8430
churn	16	0.8530	0.8660	0.8550	0.8620
churn	32	0.8460	0.8650	0.8540	0.8670
churn	64	0.8660	0.8710	0.8630	0.8650
churn	128	0.8650	0.8760	0.8640	0.8680
churn	256	0.8660	0.8940	0.8640	0.8870
churn	512	0.8660	0.9110	0.8620	0.8950
churn	1,024	0.8680	0.9330	0.8670	0.8960
cmc	8	0.3661	0.3492	0.3559	0.3356
cmc	16	0.4000	0.3492	0.3492	0.3492
cmc	32	0.4508	0.4576	0.3763	0.4407
cmc	64	0.4577	0.4847	0.4034	0.4780
cmc	128	0.4441	0.4881	0.4237	0.4746
cmc	256	0.4848	0.5119	0.3966	0.4915
cmc	512	0.5220	0.5085	0.4271	0.5017
cmc	1,024	0.4882	0.5017	0.4508	0.4949
Contaminant_10_0GHz	8	0.5479	0.5750	0.5062	0.5708
Contaminant_10_0GHz	16	0.6792	0.6625	0.5479	0.6833
Contaminant_10_0GHz	32	0.6937	0.7250	0.5563	0.7167
Contaminant_10_0GHz	64	0.7084	0.7375	0.5833	0.7604
Contaminant_10_0GHz	128	0.7354	0.8083	0.5979	0.7688
Contaminant_10_0GHz	256	0.7333	0.8292	0.6146	0.8125
Contaminant_10_0GHz	512	0.7875	0.8562	0.6271	0.8230
Contaminant_10_0GHz	1,024	0.8042	0.8750	0.5708	0.8230
Contaminant_9_5GHz	8	0.5354	0.6313	0.5042	0.6250
Contaminant_9_5GHz	16	0.6542	0.6646	0.5396	0.6771
Contaminant_9_5GHz	32	0.7188	0.7104	0.5354	0.7375
Contaminant_9_5GHz	64	0.7188	0.7500	0.5750	0.7375
Contaminant_9_5GHz	128	0.7354	0.7834	0.5875	0.7563
Contaminant_9_5GHz	256	0.7584	0.8208	0.6208	0.7875
Contaminant_9_5GHz	512	0.7937	0.8458	0.5938	0.8042
Contaminant_9_5GHz	1,024	0.8375	0.8667	0.5583	0.8042
credit_g	8	0.6050	0.6900	0.6300	0.7050
credit_g	16	0.6750	0.6850	0.6650	0.7100
credit_g	32	0.6400	0.6900	0.5850	0.7150
credit_g	64	0.6450	0.6600	0.6100	0.6850
credit_g	128	0.6750	0.7400	0.6150	0.7200
credit_g	256	0.6700	0.7650	0.6750	0.7500
credit_g	512	0.7000	0.7600	0.7100	0.7150

Continued on next page

Table 6 – continued from previous page

Dataset	Shots	KNN	RF	Qwen-2.5-7B	Our
credit_g	1,024	0.6700	0.7900	0.6650	0.7600
FICO_HELOC_cleaned	8	0.5458	0.5757	0.5175	0.5544
FICO_HELOC_cleaned	16	0.5620	0.6192	0.5094	0.6253
FICO_HELOC_cleaned	32	0.5899	0.6466	0.5403	0.6309
FICO_HELOC_cleaned	64	0.6147	0.6795	0.5129	0.6785
FICO_HELOC_cleaned	128	0.6258	0.7018	0.5215	0.6906
FICO_HELOC_cleaned	256	0.6390	0.7043	0.5276	0.7089
FICO_HELOC_cleaned	512	0.6430	0.7149	0.5256	0.6901
FICO_HELOC_cleaned	1,024	0.6512	0.7271	0.5362	0.6112
FOREX_audchf_day_High	8	0.5150	0.5123	0.5150	0.5013
FOREX_audchf_day_High	16	0.5095	0.5150	0.5422	0.5014
FOREX_audchf_day_High	32	0.5068	0.5232	0.4986	0.5123
FOREX_audchf_day_High	64	0.5341	0.5286	0.5422	0.4932
FOREX_audchf_day_High	128	0.4932	0.5259	0.5450	0.5232
FOREX_audchf_day_High	256	0.4768	0.5041	0.5613	0.5422
FOREX_audchf_day_High	512	0.4441	0.5259	0.5450	0.4959
FOREX_audchf_day_High	1,024	0.4795	0.6240	0.5395	0.5150
FOREX_audjpy_day_High	8	0.4986	0.4387	0.4496	0.4604
FOREX_audjpy_day_High	16	0.4632	0.4850	0.4550	0.4796
FOREX_audjpy_day_High	32	0.4550	0.4659	0.4578	0.4687
FOREX_audjpy_day_High	64	0.4796	0.5068	0.4796	0.4823
FOREX_audjpy_day_High	128	0.5041	0.5259	0.4959	0.5368
FOREX_audjpy_day_High	256	0.5341	0.5395	0.4659	0.5340
FOREX_audjpy_day_High	512	0.5777	0.6131	0.4932	0.6240
FOREX_audjpy_day_High	1,024	0.5531	0.6185	0.4877	0.5422
GAMETES_Heterogeneity	8	0.5281	0.5156	0.4875	0.5281
GAMETES_Heterogeneity	16	0.4875	0.5219	0.4625	0.5531
GAMETES_Heterogeneity	32	0.4750	0.5125	0.4813	0.4906
GAMETES_Heterogeneity	64	0.4656	0.5250	0.4656	0.4687
GAMETES_Heterogeneity	128	0.5125	0.4781	0.4906	0.4750
GAMETES_Heterogeneity	256	0.5437	0.5812	0.4844	0.5281
GAMETES_Heterogeneity	512	0.5781	0.5969	0.4969	0.5093
GAMETES_Heterogeneity	1,024	0.5906	0.6343	0.4938	0.5969
heloc	8	0.5315	0.5880	0.5310	0.5325
heloc	16	0.5710	0.6190	0.5085	0.6060
heloc	32	0.5975	0.6605	0.5210	0.6245
heloc	64	0.6180	0.6695	0.5250	0.6640
heloc	128	0.6375	0.6870	0.5105	0.6855
heloc	256	0.6455	0.7100	0.5105	0.6955
heloc	512	0.6555	0.7125	0.5300	0.7075
heloc	1,024	0.6575	0.7075	0.5155	0.7115
kc1	8	0.8033	0.8081	0.8104	0.7441
kc1	16	0.8152	0.8199	0.8104	0.8223
kc1	32	0.8175	0.7986	0.8175	0.7844
kc1	64	0.8176	0.8080	0.8270	0.8247
kc1	128	0.8199	0.8294	0.8341	0.8246
kc1	256	0.8246	0.8223	0.8365	0.8341
kc1	512	0.8247	0.8270	0.8341	0.8389
kc1	1,024	0.8317	0.8484	0.8365	0.8413
led24	8	0.1484	0.2203	0.0969	0.1125
led24	16	0.2094	0.2938	0.0969	0.1406
led24	32	0.3078	0.4187	0.1313	0.1531
led24	64	0.3906	0.5625	0.1266	0.2469
led24	128	0.4703	0.6187	0.1172	0.3766
led24	256	0.5375	0.6656	0.1250	0.4766
led24	512	0.5578	0.6938	0.1172	0.4844
led24	1,024	0.5922	0.7000	0.1375	0.5125
led7	8	0.2734	0.3625	0.2281	0.3219
led7	16	0.4390	0.5141	0.2609	0.4828
led7	32	0.5594	0.5766	0.3281	0.5844
led7	64	0.6562	0.6578	0.3875	0.6344

Continued on next page

Table 6 – continued from previous page

Dataset	Shots	KNN	RF	Qwen-2.5-7B	Our
led7	128	0.6875	0.6688	0.4437	0.6609
led7	256	0.6609	0.6453	0.4625	0.6422
led7	512	0.6875	0.6875	0.4844	0.6688
led7	1,024	0.7156	0.7110	0.5250	0.6438
maternal_health_risk	8	0.4089	0.4237	0.3744	0.4384
maternal_health_risk	16	0.4384	0.4877	0.4039	0.4975
maternal_health_risk	32	0.4582	0.5271	0.4532	0.5074
maternal_health_risk	64	0.5616	0.5961	0.4729	0.6108
maternal_health_risk	128	0.6503	0.6995	0.5123	0.6700
maternal_health_risk	256	0.6896	0.7439	0.5468	0.7438
maternal_health_risk	512	0.7439	0.7833	0.5961	0.7832
maternal_health_risk	1,024	0.8030	0.8276	0.5271	0.8424
pc1	8	0.9280	0.9369	0.8964	0.9189
pc1	16	0.9189	0.9189	0.8649	0.8874
pc1	32	0.9234	0.9234	0.8514	0.8874
pc1	64	0.9234	0.9324	0.9234	0.9279
pc1	128	0.9325	0.9279	0.9234	0.9279
pc1	256	0.9279	0.9459	0.9324	0.9369
pc1	512	0.9189	0.9369	0.9324	0.9324
pc1	1,024	0.9234	0.9369	0.9324	0.9280
phoneme	8	0.6337	0.6734	0.6281	0.6540
phoneme	16	0.6965	0.7280	0.6549	0.6920
phoneme	32	0.7437	0.7530	0.6698	0.7345
phoneme	64	0.7817	0.7835	0.6864	0.7484
phoneme	128	0.7909	0.7947	0.6864	0.7715
phoneme	256	0.8113	0.8252	0.6855	0.8021
phoneme	512	0.8298	0.8492	0.6873	0.8196
phoneme	1,024	0.8612	0.8650	0.6883	0.8390
Pima_Indians_Diabetes_Database	8	0.6623	0.6948	0.6429	0.6624
Pima_Indians_Diabetes_Database	16	0.6623	0.6818	0.6234	0.6883
Pima_Indians_Diabetes_Database	32	0.6493	0.7467	0.6558	0.7143
Pima_Indians_Diabetes_Database	64	0.6233	0.7272	0.6234	0.7338
Pima_Indians_Diabetes_Database	128	0.6818	0.7857	0.6818	0.7208
Pima_Indians_Diabetes_Database	256	0.7143	0.7533	0.6883	0.7338
Pima_Indians_Diabetes_Database	512	0.6883	0.7533	0.7078	0.7532
Pima_Indians_Diabetes_Database	1,024	0.7532	0.7468	0.7013	0.7402
ringnorm	8	0.5284	0.5581	0.6034	0.7230
ringnorm	16	0.5385	0.6912	0.6466	0.8987
ringnorm	32	0.5378	0.7959	0.6919	0.9324
ringnorm	64	0.5426	0.8615	0.7108	0.9520
ringnorm	128	0.5540	0.8939	0.7358	0.9541
ringnorm	256	0.5716	0.9169	0.7155	0.9628
ringnorm	512	0.5858	0.9345	0.6932	0.9595
ringnorm	1,024	0.6216	0.9358	0.7250	0.9696
rl	8	0.5181	0.5393	0.5070	0.5201
rl	16	0.5413	0.5523	0.5181	0.5332
rl	32	0.5664	0.5845	0.5392	0.5714
rl	64	0.5754	0.5905	0.5050	0.5804
rl	128	0.5946	0.5936	0.5060	0.5805
rl	256	0.5876	0.6328	0.4869	0.5966
rl	512	0.6067	0.6670	0.5181	0.6408
rl	1,024	0.6097	0.6861	0.5121	0.6278
segment	8	0.4481	0.4632	0.1970	0.4394
segment	16	0.5650	0.5390	0.2706	0.5779
segment	32	0.6364	0.6818	0.3203	0.6472
segment	64	0.7446	0.8095	0.3961	0.7684
segment	128	0.8247	0.8745	0.4113	0.8160
segment	256	0.8442	0.8961	0.4654	0.8571
segment	512	0.8810	0.9091	0.5216	0.8723
segment	1,024	0.8961	0.9156	0.4437	0.8853
seismic_bumps	8	0.9226	0.9265	0.9110	0.9246

Continued on next page

Table 6 – continued from previous page

Dataset	Shots	KNN	RF	Qwen-2.5-7B	Our
seismic_bumps	16	0.9226	0.9304	0.9284	0.9265
seismic_bumps	32	0.9323	0.9265	0.9246	0.9033
seismic_bumps	64	0.9265	0.9323	0.9304	0.9168
seismic_bumps	128	0.9303	0.9303	0.9304	0.9284
seismic_bumps	256	0.9246	0.9246	0.9304	0.9284
seismic_bumps	512	0.9284	0.9284	0.9304	0.9303
seismic_bumps	1,024	0.9265	0.9285	0.9304	0.9323
statlog	8	0.5100	0.6150	0.5350	0.5400
statlog	16	0.5400	0.6450	0.6000	0.5950
statlog	32	0.6100	0.6500	0.5750	0.6300
statlog	64	0.6350	0.6850	0.5750	0.6550
statlog	128	0.6600	0.7050	0.6250	0.6700
statlog	256	0.6850	0.7050	0.5900	0.6650
statlog	512	0.6700	0.7400	0.6300	0.6700
statlog	1,024	0.6800	0.7400	0.6300	0.7050
thyroid	8	0.9250	0.9132	0.9125	0.9139
thyroid	16	0.9257	0.9250	0.9215	0.9160
thyroid	32	0.9264	0.9277	0.9257	0.9277
thyroid	64	0.9278	0.9340	0.9243	0.9347
thyroid	128	0.9292	0.9444	0.9257	0.9396
thyroid	256	0.9361	0.9632	0.9250	0.9458
thyroid	512	0.9403	0.9798	0.9257	0.9500
thyroid	1,024	0.9438	0.9916	0.9257	0.9562
twonorm	8	0.5845	0.7155	0.4595	0.8858
twonorm	16	0.8979	0.8331	0.5230	0.9439
twonorm	32	0.9439	0.8885	0.6291	0.9500
twonorm	64	0.9547	0.9297	0.6912	0.9568
twonorm	128	0.9595	0.9446	0.7095	0.9635
twonorm	256	0.9649	0.9547	0.7318	0.9716
twonorm	512	0.9696	0.9588	0.7493	0.9750
twonorm	1,024	0.9723	0.9635	0.8000	0.9730
vehicle	8	0.3059	0.3353	0.2235	0.3647
vehicle	16	0.3824	0.4353	0.2412	0.4294
vehicle	32	0.5235	0.6000	0.3294	0.6294
vehicle	64	0.5824	0.6471	0.3706	0.6882
vehicle	128	0.5941	0.7059	0.4118	0.6588
vehicle	256	0.5706	0.7529	0.3941	0.7118
vehicle	512	0.6470	0.7471	0.3235	0.7294
vehicle	1,024	0.6529	0.7529	0.3882	0.6883
wall_robot_navigation	8	0.4332	0.5220	0.3727	0.4139
wall_robot_navigation	16	0.4716	0.5980	0.4057	0.4606
wall_robot_navigation	32	0.5138	0.7417	0.4203	0.6007
wall_robot_navigation	64	0.5604	0.8599	0.4258	0.6859
wall_robot_navigation	128	0.6181	0.9130	0.4560	0.7463
wall_robot_navigation	256	0.6722	0.9368	0.4451	0.8077
wall_robot_navigation	512	0.7344	0.9670	0.4524	0.8333
wall_robot_navigation	1,024	0.7985	0.9799	0.4762	0.8572
waveform_database_generator_version_1	8	0.4840	0.5540	0.3480	0.5480
waveform_database_generator_version_1	16	0.6330	0.6490	0.3890	0.6100
waveform_database_generator_version_1	32	0.7410	0.7270	0.3860	0.7250
waveform_database_generator_version_1	64	0.7910	0.7690	0.4140	0.7800
waveform_database_generator_version_1	128	0.7940	0.8190	0.4160	0.8060
waveform_database_generator_version_1	256	0.8120	0.7980	0.4050	0.8160
waveform_database_generator_version_1	512	0.8160	0.8270	0.4350	0.8400
waveform_database_generator_version_1	1,024	0.8220	0.8360	0.4210	0.8520
wine	8	0.6066	0.6184	0.5538	0.6281
wine	16	0.6066	0.6360	0.5499	0.6086
wine	32	0.6379	0.6458	0.5205	0.6478
wine	64	0.6477	0.6184	0.5225	0.6888
wine	128	0.6575	0.6791	0.5362	0.7006
wine	256	0.6947	0.7006	0.5714	0.7201

Continued on next page

Table 6 – continued from previous page

Dataset	Shots	KNN	RF	Qwen-2.5-7B	Our
wine	512	0.6556	0.6967	0.5616	0.7103
wine	1,024	0.6810	0.7123	0.5675	0.7260
yeast	8	0.3030	0.3401	0.2256	0.2997
yeast	16	0.3502	0.3603	0.2761	0.3434
yeast	32	0.4310	0.4175	0.3367	0.4175
yeast	64	0.4579	0.4848	0.3232	0.4949
yeast	128	0.5152	0.5185	0.2963	0.5252
yeast	256	0.5522	0.5690	0.3333	0.5522
yeast	512	0.5556	0.5825	0.3232	0.5926
yeast	1,024	0.5993	0.5993	0.3266	0.5960

Continued on next page

## C EXTENDED PER-TASK EVALUATION

Table 7: Per-dataset test accuracy from 8 to 512 shots on extended datasets in Talent. Evaluation on all 8-1024 shots and full datasets is very computation intensive, and we leave it for the next revision. Abbreviations: Qwen = Qwen-2.5-7B-Instruct; Our = MACHINELEARNINGLM (base: Qwen-2.5-7B-Instruct).

Dataset	Shots	KNN	RF	Qwen	Our
Amazon_employee_access	8	0.9254	0.9245	0.8264	0.9227
Amazon_employee_access	16	0.9221	0.9274	0.813	0.9257
Amazon_employee_access	32	0.928	0.9311	0.8407	0.9279
Amazon_employee_access	64	0.928	0.9295	0.8895	0.9266
Amazon_employee_access	128	0.9305	0.9293	0.91	0.9343
Amazon_employee_access	256	0.9276	0.9313	0.9215	0.9364
Amazon_employee_access	512	0.9291	0.9305	0.9291	0.939
BNG_breast_w	8	0.7732	0.8881	0.7915	0.921
BNG_breast_w	16	0.8894	0.9294	0.8027	0.9496
BNG_breast_w	32	0.9424	0.9409	0.8387	0.9548
BNG_breast_w	64	0.9596	0.9587	0.8538	0.959
BNG_breast_w	128	0.9666	0.9672	0.8405	0.9621
BNG_breast_w	256	0.97	0.9717	0.8455	0.9511
BNG_breast_w	512	0.9724	0.9733	0.849	0.7156
BNG_cmc	8	0.3871	0.4004	0.3691	0.3797
BNG_cmc	16	0.4029	0.4164	0.3851	0.392
BNG_cmc	32	0.4189	0.4349	0.3884	0.4199
BNG_cmc	64	0.4366	0.4586	0.3883	0.4415
BNG_cmc	128	0.4538	0.4818	0.4009	0.4769
BNG_cmc	256	0.473	0.4952	0.4062	0.4948
BNG_cmc	512	0.4855	0.5085	0.4023	0.4442
BNG_tic_tac_toe	8	0.6153	0.6018	0.529	0.5723
BNG_tic_tac_toe	16	0.6068	0.6118	0.5649	0.6012
BNG_tic_tac_toe	32	0.6152	0.6391	0.5567	0.6171
BNG_tic_tac_toe	64	0.6429	0.6645	0.5763	0.6237
BNG_tic_tac_toe	128	0.6635	0.6917	0.5837	0.6421
BNG_tic_tac_toe	256	0.6806	0.7127	0.6086	0.6545
BNG_tic_tac_toe	512	0.6971	0.7239	0.5982	0.6615
Bank_Customer_Churn_Dataset	8	0.7435	0.776	0.7105	0.731
Bank_Customer_Churn_Dataset	16	0.721	0.7765	0.7275	0.75
Bank_Customer_Churn_Dataset	32	0.725	0.79	0.744	0.767
Bank_Customer_Churn_Dataset	64	0.732	0.8045	0.757	0.787
Bank_Customer_Churn_Dataset	128	0.7485	0.816	0.7675	0.7915
Bank_Customer_Churn_Dataset	256	0.7435	0.83	0.776	0.806
Bank_Customer_Churn_Dataset	512	0.7565	0.8405	0.7935	0.8095
California_Housing_Classification	8	0.5206	0.5748	0.5301	0.6008
California_Housing_Classification	16	0.5378	0.6345	0.5434	0.6432
California_Housing_Classification	32	0.556	0.6977	0.5293	0.6953
California_Housing_Classification	64	0.5816	0.7253	0.5371	0.734

Continued on next page

Table 7 – continued from previous page

Dataset	Shots	KNN	RF	Qwen	Our
California_Housing_Classification	128	0.5919	0.7529	0.5196	0.7512
California_Housing_Classification	256	0.6085	0.7851	0.5339	0.7766
California_Housing_Classification	512	0.6107	0.8071	0.5194	0.7822
Cardiovascular_Disease_dataset	8	0.5215	0.5707	0.5624	0.5547
Cardiovascular_Disease_dataset	16	0.5338	0.6139	0.5636	0.5892
Cardiovascular_Disease_dataset	32	0.5438	0.6445	0.5681	0.6179
Cardiovascular_Disease_dataset	64	0.5458	0.6642	0.5719	0.6488
Cardiovascular_Disease_dataset	128	0.5617	0.6773	0.5705	0.6718
Cardiovascular_Disease_dataset	256	0.5694	0.6888	0.5573	0.6878
Cardiovascular_Disease_dataset	512	0.5978	0.6929	0.5559	0.6918
Click_prediction_small	8	0.7866	0.7689	0.7016	0.7029
Click_prediction_small	16	0.7883	0.7677	0.7247	0.7068
Click_prediction_small	32	0.8095	0.7964	0.7438	0.735
Click_prediction_small	64	0.816	0.8105	0.7768	0.7803
Click_prediction_small	128	0.8151	0.8172	0.7827	0.8058
Click_prediction_small	256	0.8174	0.8201	0.7863	0.8148
Click_prediction_small	512	0.8229	0.8228	0.8054	0.8239
Credit_c	8	0.4335	0.4757	0.418	0.45
Credit_c	16	0.4487	0.5232	0.4502	0.5124
Credit_c	32	0.4576	0.5602	0.4722	0.5422
Credit_c	64	0.4726	0.5895	0.5	0.5688
Credit_c	128	0.4928	0.6121	0.5013	0.5957
Credit_c	256	0.5054	0.6354	0.5246	0.6069
Credit_c	512	0.5218	0.6514	0.5288	0.6127
E_CommercShippingData	8	0.5696	0.5486	0.4991	0.5454
E_CommercShippingData	16	0.5878	0.5823	0.4995	0.5496
E_CommercShippingData	32	0.6041	0.6055	0.4932	0.5805
E_CommercShippingData	64	0.6141	0.6205	0.5159	0.6132
E_CommercShippingData	128	0.6259	0.6368	0.5054	0.6182
E_CommercShippingData	256	0.6391	0.6532	0.5127	0.6318
E_CommercShippingData	512	0.6454	0.6428	0.5204	0.6304
Employee	8	0.5715	0.5886	0.6036	0.6101
Employee	16	0.6294	0.6348	0.6079	0.6251
Employee	32	0.6208	0.6638	0.6219	0.6391
Employee	64	0.6294	0.7024	0.6402	0.6746
Employee	128	0.6702	0.7605	0.6487	0.7197
Employee	256	0.6799	0.7852	0.6477	0.7486
Employee	512	0.7025	0.8163	0.6466	0.7551
FOREX_audcad_hour_High	8	0.4965	0.501	0.5013	0.5029
FOREX_audcad_hour_High	16	0.496	0.5074	0.4943	0.506
FOREX_audcad_hour_High	32	0.4971	0.5067	0.5033	0.4968
FOREX_audcad_hour_High	64	0.5084	0.5024	0.5075	0.5171
FOREX_audcad_hour_High	128	0.5009	0.5092	0.5108	0.501
FOREX_audcad_hour_High	256	0.5077	0.5183	0.5128	0.5218
FOREX_audcad_hour_High	512	0.5101	0.5378	0.5082	0.5212
FOREX_audjpy_hour_High	8	0.5004	0.5028	0.4962	0.5006
FOREX_audjpy_hour_High	16	0.4985	0.4945	0.5061	0.4995
FOREX_audjpy_hour_High	32	0.4975	0.4909	0.5006	0.4977
FOREX_audjpy_hour_High	64	0.5013	0.4947	0.5135	0.4975
FOREX_audjpy_hour_High	128	0.507	0.504	0.4998	0.5108
FOREX_audjpy_hour_High	256	0.5044	0.5101	0.5083	0.5118
FOREX_audjpy_hour_High	512	0.5154	0.5179	0.5081	0.515
FOREX_audsgd_hour_High	8	0.5041	0.4992	0.4975	0.5033
FOREX_audsgd_hour_High	16	0.5029	0.5101	0.4995	0.5101
FOREX_audsgd_hour_High	32	0.5123	0.504	0.4941	0.5056
FOREX_audsgd_hour_High	64	0.5081	0.5081	0.5084	0.5059
FOREX_audsgd_hour_High	128	0.505	0.5024	0.5112	0.4987
FOREX_audsgd_hour_High	256	0.5178	0.5081	0.5124	0.5168
FOREX_audsgd_hour_High	512	0.5113	0.5149	0.5186	0.5103
FOREX_audusd_hour_High	8	0.506	0.4967	0.5059	0.5012
FOREX_audusd_hour_High	16	0.502	0.4934	0.5113	0.498

Continued on next page

Table 7 – continued from previous page

Dataset	Shots	KNN	RF	Qwen	Our
FOREX_audusd_hour_High	32	0.5033	0.498	0.5117	0.4962
FOREX_audusd_hour_High	64	0.5073	0.5091	0.5108	0.5097
FOREX_audusd_hour_High	128	0.5146	0.5071	0.5232	0.5112
FOREX_audusd_hour_High	256	0.5175	0.5125	0.5291	0.5111
FOREX_audusd_hour_High	512	0.5209	0.5212	0.5283	0.5159
FOREX_cadjpy_hour_High	8	0.5069	0.5018	0.5078	0.5066
FOREX_cadjpy_hour_High	16	0.5023	0.5034	0.498	0.5074
FOREX_cadjpy_hour_High	32	0.5021	0.508	0.4989	0.5068
FOREX_cadjpy_hour_High	64	0.5123	0.5058	0.5084	0.514
FOREX_cadjpy_hour_High	128	0.5042	0.5018	0.5101	0.5072
FOREX_cadjpy_hour_High	256	0.4973	0.5109	0.5099	0.5163
FOREX_cadjpy_hour_High	512	0.494	0.5128	0.5149	0.5064
Firm_Teacher_Clave_Direction_Classification	8	0.4102	0.5111	0.3694	0.3907
Firm_Teacher_Clave_Direction_Classification	16	0.5542	0.5514	0.3833	0.4829
Firm_Teacher_Clave_Direction_Classification	32	0.644	0.6143	0.4269	0.556
Firm_Teacher_Clave_Direction_Classification	64	0.6833	0.6639	0.4236	0.5986
Firm_Teacher_Clave_Direction_Classification	128	0.7125	0.7028	0.4366	0.6731
Firm_Teacher_Clave_Direction_Classification	256	0.7301	0.7273	0.4379	0.681
Firm_Teacher_Clave_Direction_Classification	512	0.7412	0.7556	0.4264	0.6648
Gender_Gap_in_Spanish_WP	8	0.4958	0.4684	0.4368	0.52
Gender_Gap_in_Spanish_WP	16	0.5095	0.5221	0.4884	0.5832
Gender_Gap_in_Spanish_WP	32	0.5316	0.5389	0.4621	0.5664
Gender_Gap_in_Spanish_WP	64	0.5053	0.5263	0.4548	0.5884
Gender_Gap_in_Spanish_WP	128	0.5358	0.5284	0.4347	0.5779
Gender_Gap_in_Spanish_WP	256	0.5442	0.5495	0.4842	0.5937
Gender_Gap_in_Spanish_WP	512	0.5558	0.5716	0.5221	0.5895
GesturePhaseSegmentationProcessed	8	0.3104	0.3104	0.2744	0.2891
GesturePhaseSegmentationProcessed	16	0.3479	0.3514	0.2532	0.3438
GesturePhaseSegmentationProcessed	32	0.4005	0.3904	0.2927	0.3489
GesturePhaseSegmentationProcessed	64	0.4299	0.438	0.2921	0.4051
GesturePhaseSegmentationProcessed	128	0.4349	0.4486	0.3078	0.4253
GesturePhaseSegmentationProcessed	256	0.439	0.4663	0.3235	0.3899
GesturePhaseSegmentationProcessed	512	0.4714	0.5073	0.3367	0.4385
HR_Analytics_Job_Change_of_Data_Scientists	8	0.6788	0.7289	0.6498	0.6738
HR_Analytics_Job_Change_of_Data_Scientists	16	0.6733	0.7369	0.6485	0.6843
HR_Analytics_Job_Change_of_Data_Scientists	32	0.6715	0.7416	0.6816	0.7098
HR_Analytics_Job_Change_of_Data_Scientists	64	0.6746	0.7484	0.6837	0.7252
HR_Analytics_Job_Change_of_Data_Scientists	128	0.6855	0.7578	0.6801	0.7333
HR_Analytics_Job_Change_of_Data_Scientists	256	0.7035	0.7724	0.6996	0.75
HR_Analytics_Job_Change_of_Data_Scientists	512	0.7103	0.7782	0.7075	0.7388
INNHotelsGroup	8	0.667	0.6286	0.5247	0.5745
INNHotelsGroup	16	0.7024	0.6713	0.5443	0.6168
INNHotelsGroup	32	0.7159	0.7027	0.5446	0.6471
INNHotelsGroup	64	0.7206	0.7344	0.5474	0.6906
INNHotelsGroup	128	0.7311	0.7591	0.5509	0.7134
INNHotelsGroup	256	0.7432	0.7796	0.5789	0.7294
INNHotelsGroup	512	0.7458	0.7976	0.5904	0.7127
Insurance	8	0.6885	0.691	0.6355	0.6609
Insurance	16	0.6794	0.6884	0.6242	0.6654
Insurance	32	0.6813	0.7097	0.6463	0.7061
Insurance	64	0.6855	0.7182	0.6419	0.7234
Insurance	128	0.6875	0.7229	0.63	0.7346
Insurance	256	0.6964	0.7244	0.6736	0.7437
Insurance	512	0.7013	0.7286	0.6605	0.748
Intersectional_Bias_Assessment	8	0.5559	0.6477	0.5091	0.5077
Intersectional_Bias_Assessment	16	0.8109	0.765	0.5177	0.5541
Intersectional_Bias_Assessment	32	0.8691	0.8236	0.5304	0.6695
Intersectional_Bias_Assessment	64	0.8941	0.8787	0.5359	0.7418
Intersectional_Bias_Assessment	128	0.9096	0.8977	0.5182	0.8145
Intersectional_Bias_Assessment	256	0.9141	0.9127	0.519	0.8314
Intersectional_Bias_Assessment	512	0.9209	0.9264	0.5318	0.8341

Continued on next page

Table 7 – continued from previous page

Dataset	Shots	KNN	RF	Qwen	Our
JapaneseVowels	8	0.1445	0.2629	0.1239	0.2223
JapaneseVowels	16	0.1751	0.3658	0.1244	0.3236
JapaneseVowels	32	0.1872	0.4947	0.133	0.4646
JapaneseVowels	64	0.2027	0.6342	0.131	0.6106
JapaneseVowels	128	0.2173	0.7486	0.1485	0.7501
JapaneseVowels	256	0.2474	0.8334	0.128	0.7963
JapaneseVowels	512	0.274	0.8786	0.137	0.842
Long	8	0.6474	0.7478	0.6496	0.6551
Long	16	0.6417	0.8359	0.6674	0.7121
Long	32	0.6306	0.8627	0.6551	0.7857
Long	64	0.6294	0.8862	0.6763	0.808
Long	128	0.6462	0.9085	0.673	0.8806
Long	256	0.6529	0.9308	0.6774	0.8303
Long	512	0.6607	0.9352	0.6897	0.865
MagicTelescope	8	0.6078	0.6104	0.5949	0.6078
MagicTelescope	16	0.6454	0.6488	0.5886	0.6861
MagicTelescope	32	0.6687	0.7119	0.6199	0.7235
MagicTelescope	64	0.6961	0.7594	0.6383	0.7603
MagicTelescope	128	0.719	0.7968	0.6364	0.7713
MagicTelescope	256	0.7403	0.8089	0.6441	0.79
MagicTelescope	512	0.75	0.8207	0.658	0.6643
PhishingWebsites	8	0.5577	0.6929	0.5658	0.6377
PhishingWebsites	16	0.7277	0.7973	0.5803	0.711
PhishingWebsites	32	0.7834	0.858	0.5889	0.7838
PhishingWebsites	64	0.8268	0.9	0.6192	0.8223
PhishingWebsites	128	0.8471	0.9068	0.6133	0.8621
PhishingWebsites	256	0.8748	0.9145	0.6432	0.8707
PhishingWebsites	512	0.8869	0.9222	0.6105	0.891
Rain_in_Australia	8	0.7417	0.7263	0.6996	0.6702
Rain_in_Australia	16	0.7583	0.7519	0.7135	0.703
Rain_in_Australia	32	0.767	0.7668	0.7209	0.7242
Rain_in_Australia	64	0.7732	0.782	0.7178	0.7486
Rain_in_Australia	128	0.775	0.79	0.717	0.7748
Rain_in_Australia	256	0.7799	0.803	0.7219	0.786
Rain_in_Australia	512	0.7828	0.8087	0.7058	0.7926
SDSS17	8	0.4949	0.6039	0.468	0.533
SDSS17	16	0.5023	0.7126	0.5077	0.6122
SDSS17	32	0.5132	0.8072	0.5296	0.6808
SDSS17	64	0.5235	0.883	0.5457	0.7328
SDSS17	128	0.5299	0.9278	0.5591	0.7722
SDSS17	256	0.5431	0.9473	0.5653	0.7976
SDSS17	512	0.5544	0.9556	0.548	0.8195
Shipping	8	0.5437	0.5423	0.4928	0.5564
Shipping	16	0.5546	0.5582	0.5045	0.5514
Shipping	32	0.5763	0.5818	0.4977	0.5827
Shipping	64	0.5827	0.6036	0.4996	0.5986
Shipping	128	0.6146	0.6218	0.4845	0.6041
Shipping	256	0.625	0.6327	0.5077	0.6036
Shipping	512	0.6255	0.6241	0.4946	0.6268
Telecom_Churn_Dataset	8	0.8531	0.859	0.8006	0.862
Telecom_Churn_Dataset	16	0.8515	0.8576	0.7781	0.8591
Telecom_Churn_Dataset	32	0.8575	0.8621	0.7886	0.8606
Telecom_Churn_Dataset	64	0.8651	0.8636	0.8051	0.8591
Telecom_Churn_Dataset	128	0.8635	0.8726	0.8081	0.8636
Telecom_Churn_Dataset	256	0.8755	0.8861	0.8156	0.8681
Telecom_Churn_Dataset	512	0.8816	0.907	0.8426	0.8696
VulNoneVul	8	0.9886	0.9868	0.9631	0.9763
VulNoneVul	16	0.9886	0.9868	0.9859	0.9798
VulNoneVul	32	0.9886	0.9886	0.9789	0.9859
VulNoneVul	64	0.9886	0.9886	0.9868	0.9886
VulNoneVul	128	0.9886	0.9886	0.9833	0.9886

Continued on next page

Table 7 – continued from previous page

Dataset	Shots	KNN	RF	Qwen	Our
VulNoneVul	256	0.9886	0.9886	0.9886	0.9886
VulNoneVul	512	0.9886	0.9886	0.9868	0.9886
Water_Quality_and_Potability	8	0.5411	0.5335	0.5671	0.4969
Water_Quality_and_Potability	16	0.5259	0.5732	0.5519	0.5686
Water_Quality_and_Potability	32	0.5442	0.5701	0.5549	0.5533
Water_Quality_and_Potability	64	0.5503	0.5747	0.5701	0.5351
Water_Quality_and_Potability	128	0.5442	0.593	0.5869	0.5869
Water_Quality_and_Potability	256	0.5366	0.5762	0.5686	0.59
Water_Quality_and_Potability	512	0.5122	0.6067	0.5945	0.5915
Wilt	8	0.9523	0.9482	0.9016	0.9451
Wilt	16	0.9472	0.9347	0.8829	0.9461
Wilt	32	0.9513	0.944	0.912	0.9462
Wilt	64	0.9544	0.9544	0.9254	0.9388
Wilt	128	0.9523	0.9565	0.9295	0.9617
Wilt	256	0.9544	0.9627	0.941	0.9689
Wilt	512	0.9596	0.97	0.9482	0.9741
abalone	8	0.4294	0.4809	0.3947	0.4629
abalone	16	0.4785	0.5095	0.3971	0.5096
abalone	32	0.5167	0.5239	0.3708	0.5371
abalone	64	0.5455	0.5383	0.3768	0.5299
abalone	128	0.5634	0.555	0.4174	0.5706
abalone	256	0.5933	0.5694	0.3888	0.5718
abalone	512	0.6088	0.5993	0.4653	0.6017
ada_prior	8	0.6528	0.7043	0.7262	0.7306
ada_prior	16	0.6594	0.7327	0.7426	0.7415
ada_prior	32	0.6408	0.7491	0.7591	0.7426
ada_prior	64	0.6835	0.7765	0.7524	0.7656
ada_prior	128	0.6879	0.7962	0.7601	0.7821
ada_prior	256	0.7031	0.793	0.7568	0.7908
ada_prior	512	0.6999	0.8247	0.7371	0.805
adult	8	0.6705	0.7319	0.7313	0.7344
adult	16	0.6785	0.7531	0.7485	0.7579
adult	32	0.6908	0.7734	0.7737	0.766
adult	64	0.6946	0.7959	0.7674	0.7761
adult	128	0.708	0.8098	0.7736	0.791
adult	256	0.7095	0.8197	0.7713	0.7985
adult	512	0.7162	0.8337	0.7651	0.8174
airlines_seed_0_nrows_2000_nclasses_10_ncols_100	8	0.51	0.54	0.9285	0.5375
airlines_seed_0_nrows_2000_nclasses_10_ncols_100	16	0.5075	0.52	0.9325	0.515
airlines_seed_0_nrows_2000_nclasses_10_ncols_100	32	0.4725	0.5125	0.9471	0.51
airlines_seed_0_nrows_2000_nclasses_10_ncols_100	64	0.5	0.5075	0.9364	0.495
airlines_seed_0_nrows_2000_nclasses_10_ncols_100	128	0.535	0.56	0.9471	0.5275
airlines_seed_0_nrows_2000_nclasses_10_ncols_100	256	0.535	0.59	0.9483	0.54
airlines_seed_0_nrows_2000_nclasses_10_ncols_100	512	0.5175	0.5575	0.57	0.5475
allbp	8	0.9431	0.943	0.9484	0.9496
allbp	16	0.9536	0.9523	0.9351	0.951
allbp	32	0.9536	0.955	0.8954	0.9523
allbp	64	0.9536	0.9563	0.943	0.9536
allbp	128	0.9536	0.9576	0.9563	0.9563
allbp	256	0.9576	0.9563	0.955	0.9563
allbp	512	0.9603	0.9669	0.951	0.9523
artificial_characters	8	0.1595	0.16	0.1135	0.1477
artificial_characters	16	0.184	0.1854	0.1154	0.1786
artificial_characters	32	0.227	0.2446	0.1389	0.2148
artificial_characters	64	0.2994	0.3068	0.1453	0.2794
artificial_characters	128	0.3591	0.4095	0.1771	0.3576
artificial_characters	256	0.4193	0.4731	0.205	0.4095
artificial_characters	512	0.4594	0.5259	0.1937	0.4618
compass	8	0.532	0.5554	0.5173	0.5389
compass	16	0.5614	0.5678	0.5296	0.5551
compass	32	0.5816	0.6176	0.5425	0.5918

Continued on next page

Table 7 – continued from previous page

Dataset	Shots	KNN	RF	Qwen	Our
compass	64	0.5843	0.6254	0.5458	0.5978
compass	128	0.5788	0.6416	0.541	0.6326
compass	256	0.6056	0.6575	0.5455	0.6435
compass	512	0.6098	0.6606	0.5293	0.6419
connect_4	8	0.6032	0.5793	0.5593	0.6055
connect_4	16	0.6122	0.6011	0.6038	0.618
connect_4	32	0.6147	0.6152	0.6171	0.6315
connect_4	64	0.6139	0.6334	0.6246	0.6417
connect_4	128	0.6181	0.6429	0.64	0.6322
connect_4	256	0.621	0.6622	0.6483	0.643
connect_4	512	0.6282	0.6762	0.653	0.65
credit	8	0.5073	0.5375	0.4986	0.571
credit	16	0.5121	0.5558	0.5178	0.6156
credit	32	0.5214	0.5881	0.5186	0.6539
credit	64	0.5139	0.6174	0.5238	0.6826
credit	128	0.5166	0.6357	0.5283	0.7152
credit	256	0.5178	0.6428	0.5328	0.7197
credit	512	0.5059	0.6533	0.5151	0.7248
customer_satisfaction_in_airline	8	0.5158	0.6521	0.5669	0.5982
customer_satisfaction_in_airline	16	0.5242	0.7118	0.5964	0.6621
customer_satisfaction_in_airline	32	0.5368	0.7682	0.6067	0.74
customer_satisfaction_in_airline	64	0.5451	0.8106	0.5961	0.7777
customer_satisfaction_in_airline	128	0.5536	0.8412	0.6107	0.7994
customer_satisfaction_in_airline	256	0.559	0.8646	0.6193	0.8113
customer_satisfaction_in_airline	512	0.565	0.883	0.5726	0.8294
dabetes_130_us_hospitals	8	0.4986	0.5214	0.5231	0.497
dabetes_130_us_hospitals	16	0.5083	0.5215	0.5298	0.5032
dabetes_130_us_hospitals	32	0.5099	0.5397	0.5323	0.5119
dabetes_130_us_hospitals	64	0.5139	0.5449	0.5353	0.5246
dabetes_130_us_hospitals	128	0.5166	0.557	0.5283	0.5419
dabetes_130_us_hospitals	256	0.5187	0.5742	0.5346	0.5474
dabetes_130_us_hospitals	512	0.5221	0.5868	0.5288	0.5518
default_of_credit_card_clients	8	0.7355	0.7335	0.6715	0.6913
default_of_credit_card_clients	16	0.7432	0.7535	0.6756	0.7298
default_of_credit_card_clients	32	0.7354	0.7582	0.7177	0.7244
default_of_credit_card_clients	64	0.7437	0.7756	0.7456	0.7723
default_of_credit_card_clients	128	0.7414	0.7919	0.7478	0.7849
default_of_credit_card_clients	256	0.7463	0.798	0.7588	0.7995
default_of_credit_card_clients	512	0.7486	0.802	0.764	0.7819
delta_ailerons	8	0.6851	0.7686	0.5301	0.758
delta_ailerons	16	0.744	0.866	0.5533	0.7763
delta_ailerons	32	0.8233	0.9088	0.5406	0.8654
delta_ailerons	64	0.8843	0.9166	0.5617	0.8885
delta_ailerons	128	0.9096	0.9243	0.5652	0.9005
delta_ailerons	256	0.9187	0.9257	0.6052	0.9004
delta_ailerons	512	0.9242	0.9327	0.5743	0.92
dry_beans_dataset	8	0.3992	0.5237	0.227	0.455
dry_beans_dataset	16	0.4741	0.6739	0.267	0.6287
dry_beans_dataset	32	0.5207	0.765	0.3092	0.7664
dry_beans_dataset	64	0.5476	0.8281	0.3606	0.8061
dry_beans_dataset	128	0.5762	0.8652	0.426	0.8358
dry_beans_dataset	256	0.5832	0.8818	0.4815	0.8656
dry_beans_dataset	512	0.6049	0.8931	0.5094	0.8329
eeg_eye_state	8	0.511	0.5391	0.525	0.5157
eeg_eye_state	16	0.5487	0.5481	0.528	0.5261
eeg_eye_state	32	0.5721	0.5718	0.5254	0.5277
eeg_eye_state	64	0.6015	0.6202	0.5451	0.5801
eeg_eye_state	128	0.6752	0.6562	0.5384	0.6155
eeg_eye_state	256	0.7447	0.6852	0.5464	0.6812
eeg_eye_state	512	0.8021	0.747	0.548	0.716
electricity	8	0.5282	0.6019	0.5937	0.5696

Continued on next page

Table 7 – continued from previous page

Dataset	Shots	KNN	RF	Qwen	Our
electricity	16	0.53	0.6489	0.5952	0.6126
electricity	32	0.5396	0.6945	0.603	0.6654
electricity	64	0.5553	0.7169	0.6158	0.6925
electricity	128	0.5795	0.7411	0.6225	0.7056
electricity	256	0.6172	0.7622	0.6142	0.7304
electricity	512	0.6376	0.7728	0.6152	0.7458
eye_movements	8	0.3548	0.3633	0.3436	0.337
eye_movements	16	0.3634	0.3771	0.3535	0.3522
eye_movements	32	0.3653	0.3817	0.3568	0.366
eye_movements	64	0.3693	0.4021	0.3594	0.4034
eye_movements	128	0.3817	0.431	0.3436	0.4192
eye_movements	256	0.4061	0.4573	0.3555	0.41
eye_movements	512	0.3956	0.4718	0.343	0.4409
eye_movements_bin	8	0.4973	0.4993	0.4816	0.4974
eye_movements_bin	16	0.4869	0.4921	0.5072	0.4796
eye_movements_bin	32	0.5046	0.5	0.4796	0.4757
eye_movements_bin	64	0.5125	0.5197	0.477	0.4869
eye_movements_bin	128	0.5453	0.5243	0.4882	0.5328
eye_movements_bin	256	0.5303	0.523	0.4764	0.5138
eye_movements_bin	512	0.5309	0.546	0.4915	0.5152
house_16H	8	0.6064	0.6334	0.4922	0.5771
house_16H	16	0.6486	0.7187	0.5015	0.6442
house_16H	32	0.6646	0.7517	0.4967	0.6839
house_16H	64	0.6567	0.7865	0.513	0.7135
house_16H	128	0.6708	0.8065	0.5048	0.7231
house_16H	256	0.6686	0.8184	0.5204	0.7717
house_16H	512	0.676	0.8262	0.5152	0.7413
in_vehicle_coupon_recommendation	8	0.5207	0.5205	0.4927	0.5089
in_vehicle_coupon_recommendation	16	0.5353	0.5345	0.4888	0.5277
in_vehicle_coupon_recommendation	32	0.5199	0.5412	0.5002	0.5483
in_vehicle_coupon_recommendation	64	0.5412	0.5664	0.4982	0.5309
in_vehicle_coupon_recommendation	128	0.5408	0.5605	0.4841	0.5306
in_vehicle_coupon_recommendation	256	0.5613	0.6042	0.5211	0.5577
in_vehicle_coupon_recommendation	512	0.5712	0.6437	0.5124	0.5692
internet_firewall	8	0.7062	0.7704	0.5475	0.7163
internet_firewall	16	0.8121	0.8463	0.6043	0.7863
internet_firewall	32	0.8669	0.8898	0.6278	0.7993
internet_firewall	64	0.8908	0.9105	0.6365	0.8101
internet_firewall	128	0.9099	0.9242	0.6446	0.8031
internet_firewall	256	0.921	0.9323	0.6133	0.7941
internet_firewall	512	0.9245	0.9327	0.5876	0.7995
jm1	8	0.7781	0.7607	0.7423	0.7217
jm1	16	0.7804	0.7772	0.7658	0.7478
jm1	32	0.7754	0.7827	0.7818	0.7606
jm1	64	0.7731	0.7915	0.7869	0.7754
jm1	128	0.779	0.7979	0.7997	0.8002
jm1	256	0.7851	0.7869	0.813	0.8062
jm1	512	0.7998	0.8011	0.8089	0.8209
jungle_chess_2pcs_raw_endgame_complete	8	0.5064	0.5282	0.4732	0.4986
jungle_chess_2pcs_raw_endgame_complete	16	0.5851	0.5868	0.5069	0.5723
jungle_chess_2pcs_raw_endgame_complete	32	0.6188	0.629	0.5116	0.6074
jungle_chess_2pcs_raw_endgame_complete	64	0.6523	0.6713	0.5227	0.6405
jungle_chess_2pcs_raw_endgame_complete	128	0.672	0.7033	0.5422	0.6785
jungle_chess_2pcs_raw_endgame_complete	256	0.6961	0.7392	0.5462	0.7001
jungle_chess_2pcs_raw_endgame_complete	512	0.7317	0.7615	0.5543	0.6779
kdd_ipums_la_97_small	8	0.5963	0.6686	0.5617	0.63
kdd_ipums_la_97_small	16	0.6715	0.7755	0.5915	0.7052
kdd_ipums_la_97_small	32	0.7042	0.8199	0.605	0.763
kdd_ipums_la_97_small	64	0.7746	0.8275	0.6435	0.7987
kdd_ipums_la_97_small	128	0.8025	0.8343	0.5896	0.7688
kdd_ipums_la_97_small	256	0.8064	0.8565	0.5839	0.7871

Continued on next page

Table 7 – continued from previous page

Dataset	Shots	KNN	RF	Qwen	Our
kdd_ipums_la_97_small	512	0.8218	0.8468	0.5829	0.7033
kr_vs_kp	8	0.5	0.5531	0.4734	0.5219
kr_vs_kp	16	0.5703	0.6141	0.4672	0.5344
kr_vs_kp	32	0.7219	0.7422	0.5109	0.6109
kr_vs_kp	64	0.7281	0.8422	0.4875	0.6547
kr_vs_kp	128	0.7797	0.925	0.5234	0.725
kr_vs_kp	256	0.8359	0.9578	0.5203	0.75
kr_vs_kp	512	0.8562	0.9656	0.5359	0.7641
kropt	8	0.1354	0.1431	0.0882	0.0699
kropt	16	0.1454	0.1623	0.087	0.0661
kropt	32	0.1725	0.1855	0.0775	0.0665
kropt	64	0.2015	0.2201	0.077	0.0624
kropt	128	0.2363	0.2651	0.0823	0.0764
kropt	256	0.2753	0.3282	0.083	0.1005
kropt	512	0.3175	0.379	0.0752	0.1162
law_school_admission_bianry	8	0.6377	0.7245	0.6048	0.6738
law_school_admission_bianry	16	0.6538	0.8238	0.6365	0.7413
law_school_admission_bianry	32	0.6447	0.9279	0.6565	0.7996
law_school_admission_bianry	64	0.6483	0.982	0.7058	0.8642
law_school_admission_bianry	128	0.6714	0.9971	0.717	0.9029
law_school_admission_bianry	256	0.6822	0.9998	0.7414	0.925
law_school_admission_bianry	512	0.693	1	0.7685	0.9437
letter	8	0.0825	0.109	0.0398	0.0383
letter	16	0.132	0.156	0.0387	0.0375
letter	32	0.184	0.228	0.0375	0.0462
letter	64	0.2665	0.3377	0.0425	0.068
letter	128	0.3688	0.4742	0.044	0.127
letter	256	0.488	0.616	0.042	0.1777
letter	512	0.605	0.718	0.039	0.215
mammography	8	0.9772	0.9772	0.9472	0.9567
mammography	16	0.9772	0.9763	0.9625	0.9597
mammography	32	0.9772	0.9759	0.9566	0.9665
mammography	64	0.9767	0.9763	0.9687	0.9687
mammography	128	0.9781	0.9808	0.9705	0.9759
mammography	256	0.9803	0.9826	0.9678	0.9812
mammography	512	0.9821	0.9848	0.9723	0.983
microaggregation2	8	0.4627	0.436	0.417	0.3815
microaggregation2	16	0.4627	0.468	0.4475	0.436
microaggregation2	32	0.4895	0.4748	0.4733	0.4945
microaggregation2	64	0.5033	0.5102	0.491	0.5238
microaggregation2	128	0.519	0.5188	0.503	0.5375
microaggregation2	256	0.518	0.535	0.523	0.5385
microaggregation2	512	0.5218	0.5465	0.5393	0.551
mobile_c36_oversampling	8	0.6599	0.6687	0.5412	0.6654
mobile_c36_oversampling	16	0.7128	0.7639	0.5549	0.7429
mobile_c36_oversampling	32	0.7902	0.8164	0.5759	0.7937
mobile_c36_oversampling	64	0.8269	0.8513	0.6104	0.825
mobile_c36_oversampling	128	0.8485	0.8735	0.6309	0.8474
mobile_c36_oversampling	256	0.8669	0.8899	0.6525	0.8667
mobile_c36_oversampling	512	0.8854	0.9011	0.6751	0.8838
mozilla4	8	0.6822	0.7533	0.6057	0.7089
mozilla4	16	0.7507	0.8636	0.6224	0.7668
mozilla4	32	0.7932	0.8945	0.6494	0.7951
mozilla4	64	0.8205	0.9051	0.6825	0.834
mozilla4	128	0.8546	0.9218	0.6687	0.8523
mozilla4	256	0.8749	0.9267	0.6822	0.8575
mozilla4	512	0.8852	0.9306	0.6536	0.6208
national_longitudinal_survey_binary	8	0.5855	0.7271	0.6059	0.5377
national_longitudinal_survey_binary	16	0.5896	0.8584	0.6029	0.5968
national_longitudinal_survey_binary	32	0.6222	0.9399	0.6283	0.6446
national_longitudinal_survey_binary	64	0.6273	0.9827	0.6456	0.6843

Continued on next page

Table 7 – continued from previous page

Dataset	Shots	KNN	RF	Qwen	Our
national_longitudinal_survey_binary	128	0.6283	0.9939	0.6456	0.7465
national_longitudinal_survey_binary	256	0.6436	0.998	0.6467	0.7597
national_longitudinal_survey_binary	512	0.6426	0.998	0.6558	0.8065
okcupid_stem	8	0.6824	0.6793	0.6374	0.6079
okcupid_stem	16	0.6887	0.6769	0.6419	0.657
okcupid_stem	32	0.6884	0.6807	0.6488	0.6752
okcupid_stem	64	0.6902	0.696	0.6477	0.6968
okcupid_stem	128	0.6964	0.6996	0.6778	0.711
okcupid_stem	256	0.6955	0.706	0.6726	0.7155
okcupid_stem	512	0.688	0.7135	0.6747	0.7135
online_shoppers	8	0.854	0.8447	0.7137	0.7891
online_shoppers	16	0.8573	0.852	0.6833	0.8269
online_shoppers	32	0.8686	0.858	0.8086	0.8362
online_shoppers	64	0.8763	0.8718	0.7977	0.854
online_shoppers	128	0.8824	0.8791	0.8025	0.8654
online_shoppers	256	0.8873	0.884	0.8285	0.8763
online_shoppers	512	0.8917	0.8917	0.8321	0.8844
page_blocks	8	0.8822	0.8904	0.821	0.8356
page_blocks	16	0.8868	0.8959	0.8156	0.8521
page_blocks	32	0.8868	0.8996	0.8648	0.8886
page_blocks	64	0.8922	0.9178	0.8639	0.9114
page_blocks	128	0.8959	0.9297	0.8803	0.9133
page_blocks	256	0.9087	0.9407	0.8777	0.9306
page_blocks	512	0.9251	0.9535	0.8822	0.9398
pendigits	8	0.2865	0.326	0.1073	0.2628
pendigits	16	0.4279	0.4529	0.1323	0.4443
pendigits	32	0.5925	0.6362	0.1514	0.6367
pendigits	64	0.7408	0.7776	0.171	0.7781
pendigits	128	0.8436	0.8467	0.1792	0.8276
pendigits	256	0.8963	0.9086	0.2278	0.8872
pendigits	512	0.9359	0.9418	0.2178	0.8608
pol	8	0.5548	0.5627	0.5052	0.5305
pol	16	0.6113	0.6411	0.5101	0.5791
pol	32	0.6743	0.7888	0.5251	0.7025
pol	64	0.7506	0.8533	0.5196	0.7764
pol	128	0.7928	0.9063	0.5448	0.8547
pol	256	0.8414	0.9281	0.5543	0.8904
pol	512	0.8686	0.9395	0.5538	0.8394
rice_cammemo_and_osmancik	8	0.769	0.8491	0.5407	0.7939
rice_cammemo_and_osmancik	16	0.8491	0.8858	0.6457	0.8504
rice_cammemo_and_osmancik	32	0.8583	0.891	0.6706	0.8478
rice_cammemo_and_osmancik	64	0.8662	0.9134	0.7612	0.8937
rice_cammemo_and_osmancik	128	0.8635	0.916	0.7703	0.8976
rice_cammemo_and_osmancik	256	0.8675	0.9081	0.7743	0.9029
rice_cammemo_and_osmancik	512	0.8806	0.9081	0.811	0.8058
shill_bidding	8	0.8822	0.8656	0.845	0.8205
shill_bidding	16	0.8759	0.8814	0.8466	0.838
shill_bidding	32	0.8704	0.8799	0.8348	0.8553
shill_bidding	64	0.8885	0.8775	0.8553	0.8775
shill_bidding	128	0.8798	0.879	0.8727	0.8838
shill_bidding	256	0.8814	0.8735	0.8672	0.8877
shill_bidding	512	0.8861	0.8751	0.8783	0.8973
shruntime	8	0.7465	0.747	0.6965	0.732
shruntime	16	0.75	0.775	0.7425	0.7665
shruntime	32	0.7445	0.7935	0.756	0.7835
shruntime	64	0.741	0.803	0.7695	0.789
shruntime	128	0.7365	0.8155	0.774	0.7965
shruntime	256	0.743	0.825	0.7875	0.8125
shruntime	512	0.753	0.84	0.792	0.824
shuttle	8	0.7998	0.8302	0.6834	0.7713
shuttle	16	0.8209	0.8661	0.7357	0.8181

Continued on next page

Table 7 – continued from previous page

Dataset	Shots	KNN	RF	Qwen	Our
shuttle	32	0.8523	0.9063	0.7641	0.876
shuttle	64	0.8956	0.958	0.7905	0.9319
shuttle	128	0.9443	0.9873	0.8018	0.9541
shuttle	256	0.9706	0.9941	0.7899	0.9626
shuttle	512	0.9818	0.9952	0.8112	0.8215
splice	8	0.4624	0.4608	0.4107	0.4671
splice	16	0.4624	0.5204	0.3887	0.4467
splice	32	0.5094	0.6269	0.4828	0.5
splice	64	0.5344	0.7053	0.4294	0.5047
splice	128	0.5643	0.79	0.4749	0.5203
splice	256	0.6191	0.8511	0.4546	0.5345
splice	512	0.6724	0.906	0.4874	0.5298
sylvine	8	0.5073	0.599	0.6068	0.5571
sylvine	16	0.5444	0.7434	0.6215	0.6693
sylvine	32	0.5697	0.8263	0.601	0.7395
sylvine	64	0.5707	0.882	0.6098	0.8078
sylvine	128	0.6107	0.8858	0.6644	0.8283
sylvine	256	0.6683	0.9063	0.6547	0.8556
sylvine	512	0.7073	0.9073	0.5991	0.84
telco_customer_churn	8	0.7161	0.6834	0.6452	0.6387
telco_customer_churn	16	0.7218	0.7303	0.6899	0.6742
telco_customer_churn	32	0.7303	0.7303	0.6707	0.7189
telco_customer_churn	64	0.7608	0.7814	0.7069	0.7587
telco_customer_churn	128	0.7616	0.7814	0.6991	0.7637
telco_customer_churn	256	0.7573	0.7722	0.7005	0.7714
telco_customer_churn	512	0.7665	0.7843	0.6934	0.7842
texture	8	0.0375	0.0375	0.1273	0.2118
texture	16	0.0625	0.05	0.1709	0.2664
texture	32	0.0844	0.0625	0.1964	0.3927
texture	64	0.1	0.0969	0.21	0.53
texture	128	0.1906	0.2437	0.2427	0.6464
texture	256	0.3781	0.3563	0.2436	0.6455
texture	512	0.4844	0.5312	0.2365	0.6506
thyroid_ann	8	0.9033	0.9298	0.8781	0.9272
thyroid_ann	16	0.9205	0.9245	0.9179	0.9245
thyroid_ann	32	0.9178	0.9391	0.9192	0.9324
thyroid_ann	64	0.9179	0.947	0.9086	0.9245
thyroid_ann	128	0.9179	0.9537	0.9179	0.9325
thyroid_ann	256	0.9206	0.9589	0.9166	0.9073
thyroid_ann	512	0.9232	0.9762	0.9231	0.9232
thyroid_dis	8	0.5464	0.5607	0.4268	0.4553
thyroid_dis	16	0.55	0.5893	0.4179	0.5625
thyroid_dis	32	0.5322	0.5947	0.5018	0.5875
thyroid_dis	64	0.5268	0.6464	0.4947	0.65
thyroid_dis	128	0.5464	0.6661	0.4304	0.6411
thyroid_dis	256	0.5947	0.6964	0.4929	0.6768
thyroid_dis	512	0.5768	0.7036	0.3929	0.6572
turiye_student_evaluation	8	0.2646	0.2466	0.2294	0.238
turiye_student_evaluation	16	0.2655	0.2835	0.2388	0.25
turiye_student_evaluation	32	0.3127	0.3359	0.2543	0.2809
turiye_student_evaluation	64	0.3497	0.3858	0.2809	0.3127
turiye_student_evaluation	128	0.3823	0.4304	0.2843	0.3634
turiye_student_evaluation	256	0.4004	0.4399	0.3016	0.3832
turiye_student_evaluation	512	0.4098	0.4587	0.3033	0.4175
walking_activity	8	0.1241	0.1355	0.0192	0.0138
walking_activity	16	0.14	0.1702	0.0175	0.0092
walking_activity	32	0.1502	0.2148	0.0164	0.0089
walking_activity	64	0.166	0.2593	0.0154	0.0135
walking_activity	128	0.1848	0.3094	0.0173	0.0267
walking_activity	256	0.2169	0.3573	0.0167	0.0508
walking_activity	512	0.2577	0.4078	0.0155	0.0629

Continued on next page

Table 7 – continued from previous page

Dataset	Shots	KNN	RF	Qwen	Our
water_quality	8	0.8856	0.8763	0.8275	0.8619
water_quality	16	0.8857	0.8694	0.8294	0.8644
water_quality	32	0.8819	0.8781	0.8656	0.8688
water_quality	64	0.8825	0.8782	0.8469	0.8807
water_quality	128	0.8819	0.8775	0.8531	0.885
water_quality	256	0.8813	0.8769	0.8737	0.8893
water_quality	512	0.8819	0.8825	0.8737	0.8907
wine_quality_white	8	0.3694	0.4051	0.3429	0.3296
wine_quality_white	16	0.3908	0.4163	0.3888	0.3929
wine_quality_white	32	0.4031	0.4561	0.3939	0.4459
wine_quality_white	64	0.4194	0.4663	0.4306	0.4337
wine_quality_white	128	0.4072	0.4888	0.4245	0.4439
wine_quality_white	256	0.4439	0.4867	0.4234	0.4806
wine_quality_white	512	0.4541	0.5224	0.402	0.5071